Photochemical Advanced Oxidation Processes for Water and Wastewater Treatment

Marta I. Litter*[1,2,3] and Natalia Quici[4]

[1]*Gerencia Química, Comisión Nacional de Energía Atómica, San Martín, Prov. de Buenos Aires, Argentina,* [2]*Consejo Nacional de Investigaciones Científicas y Técnicas, Buenos Aires, Argentina,* [3]*Universidad Nacional de Gral. San Martín, San Martín, Prov. de Buenos Aires, Argentina,* [4]*Photocatalysis and Photoreaction Engineering, Department of Chemical and Environmental Engineering, The University of Nottingham, Nottingham, UK*

Abstract: Advanced Oxidation Processes (AOPs) are excellent systems for remediation of contaminated wastewaters containing recalcitrant organic pollutants. The most studied AOPs are photochemical-based processes (PAOPs), as UV/hydrogen peroxide, heterogeneous photocatalysis (HP), photo-Fenton (PF), UV plus ozone and combination of these technologies. All AOPs are based on the production of very reactive species (especially hydroxyl radicals, HO$^\bullet$) able to degrade or transform chemical pollutants, provoking ultimately total mineralization. One of the major drawbacks of AOPs is that the operational costs are relatively high compared to less expensive technologies such as biological treatments, use of activated carbon, etc. However, these technologies can be used combined with themselves or with conventional technologies. In spite of a huge amount of scientific publications, applications and patented methods on PAOPs are scarce. In this article, a brief review on the most used PAOPs, together with recent patents on the field are presented. The patents describe mostly inventions on HP and PF, most of them using catalysts supported on membranes, perovskites, zeolites or other materials, and combination of PAOPs with conventional technologies.

1. INTRODUCTION

Historically, different methods have been used for treatment of industrial and domestic wastewaters, drinking water purification and disinfection, ultrapurification of water for especial uses (pharmaceutics or microelectronics), etc. In most cases, anthropogenically polluted water can be effectively treated by conventional methods, such as biological processes, adsorption on activated carbon or other materials, thermal oxidation, chlorination, ozonation, flocculation-precipitation, reverse osmosis (RO), etc. However, in some cases, conventional procedures are not adequate to reach the degree of purity required by international or local regulations or by the subsequent use of the effluent. In these cases, Advanced Oxidation Processes (AOPs) or Advanced Oxidation Technologies (AOTs) are efficient novel methods for water treatment that permit the total or partial elimination of compounds resistant to conventional treatments, reduction of toxicity or destruction of pathogen microorganisms.

AOPs are based on physicochemical processes that produce powerful oxidative species like the hydroxyl radical (HO$^\bullet$), whose standard redox potential is 2.8 V[1].

Other reactive oxygen species (ROS) like HO$^\bullet$, O$_2^{\bullet-}$/HO$_2^\bullet$, H$_2$O$_2$ are also formed and contribute to the redox processes enabling the transformation of the target pollutant. Depending on the physicochemical process leading to the formation of these species, AOPs can be divided into non-photochemical and photochemical processes. If light irradiation of low UV-visible fluence is provided, the second group would require less energy consumption and fewer amounts of chemicals than the second type of processes. Thus, photochemical processes are at present more widely employed. Most common AOPs are listed in Table **1**.

Hydroxyl radicals formed in AOPs react principally *via* hydrogen abstraction (eq. (1)), electrophilic addition to π systems (eq. (2)), and electron transfer reactions (eq. (3)) [1]:

$$HO^\bullet + RH \rightarrow R^\bullet + H_2O \tag{1}$$

$$HO^\bullet + ArX \rightarrow HOArX^\bullet \tag{2}$$

$$HO^\bullet + RX \rightarrow RX^{\bullet+} + HO^- \tag{3}$$

where R represents an aliphatic chain and Ar an aromatic group. In the case of aromatic compounds, a hydroxylation of the ring might occur with a subsequent ring opening after successive HO$^\bullet$ attacks, giving place to conjugated structures or organic acids. In every case, the process can lead to the total mineralization of the compound.

AOPs are developed and commercialized to a variable degree and are undergoing constant change as technological advances take place. At present, UV/H$_2$O$_2$, UV/O$_3$,

Address correspondence to this author at Gerencia Química, Comisión Nacional de Energía Atómica, Av. Gral. Paz 1499, 1650 San Martín, Prov. de Buenos Aires, Argentina; Tel: +5411 6772 7016; Fax: +5411 6772 7886; E-mail: litter@cnea.gov.ar

---

[1] All standard reduction potentials given in this work are vs. NHE.

Table 1.   Advanced Oxidation Processes

Non-Photochemical Processes	Photochemical Processes	
	Type of Process	Irradiation Wavelength Range (λ/nm)
Alkaline ozonation (O_3/HO^-)	Water photolysis in vacuum ultraviolet (VUV)	< 190
Ozonation with hydrogen peroxide (O_3/H_2O_2)	UV/hydrogen peroxide (UV/H_2O_2)	< 280
Fenton and related processes (Fe^{2+}/H_2O_2)	UV/ozone (UV/O_3)	280-315
Electrochemical oxidation	Photo-Fenton (PF) and related processes	UV-Vis up to 450
γ-Radiolysis and electron-beam treatment	Zerovalent iron plus UV light	UV range
Non-thermal plasma (surface corona discharge)	Heterogeneous photocatalysis (HP) using TiO_2	UV: up to 380-400
Electrohydraulic discharge-ultrasound (US, cavitation)		
Wet air oxidation		
Supercritical water oxidation		
Zerovalent iron (ZVI)		
Ferrate		

UV/H_2O_2/O_3, PF and HP are totally or partially commercialized.

This review will focus on the description and advances related with main PAOPs from last years (ca. 2005), treating only those technologies mentioned in recent patents. The article will include studies of combination of individual AOPs and examples of patents. Previous revisions on the subject, including AOPs not cited here can be found, for example, in references [2-14].

2. PHOTOCHEMICAL ADVANCED OXIDATION PROCESSES

2.1. UV/H_2O_2

The oxidizing power of hydrogen peroxide can be sensibly improved by $HO^\bullet$ generation through cleavage of the O-O union with photons of high energy (λ < 280 nm) [11]. The reaction has a low quantum yield ($\varphi_{HO^\bullet}$ = 0.5) due to rapid recombination of the radicals in solution, and produces almost quantitatively one $HO^\bullet$ per quantum of radiation absorbed in the 200-300 nm range:

$$H_2O_2 + h\nu \rightarrow 2\ HO^\bullet \qquad (4)$$

H_2O_2 photolysis is usually performed with low- or medium-pressure mercury vapor lamps. Almost 50% of the energetic consumption is lost in the form of heat or emissions less than 185 nm, which are absorbed by the quartz jacket. Generally, cheap germicidal lamps are used; however, since H_2O_2 absorption is maximal at 220 nm, it is more convenient to use Xe/Hg lamps that - although more expensive - emit in the 210-240 nm range.

In addition to H_2O_2 (ε = 18.6 M^{-1} cm^{-1} at 254 nm), other species can absorb photons at these short wavelengths, and they can act as light filters. However, if the contaminants can be directly photolyzed, this may improve the efficiency of the oxidative destruction process. Since the intensity of UV

radiation decays exponentially towards the bulk of the solution, it is necessary to establish conditions of turbulent flow to renew continuously the solution surrounding the luminous source. The UV fluence rate [15] varies with distance from the lamp and it is a function of the absorptive characteristics of the media through which the UV radiation passes. Both the organic contaminant and H_2O_2 may absorb UV radiation, reducing the transmitted fluence rate and changing the effectiveness of $HO^\bullet$ production throughout the photoreactor. Reflection, refraction, shadowing, and lamp characteristics influence also the radiant power distribution within a UV reactor [16].
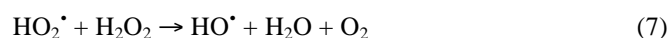
In the presence of oxygen and organic compounds, multiple pathways are operative in the UV/H_2O_2 system involving the generation of hydroxyl, organic and organic peroxyl radicals [5].

In alkaline media, the photochemical process is more efficient since the concentration of the conjugate anion of hydrogen peroxide increases with pH (eq. (5)), and this species has a higher absorption coefficient (ε_{254} = 240 M^{-1} cm^{-1}) than H_2O_2, favoring light absorption and increasing $HO^\bullet$ production [5].

$$H_2O_2 \rightleftarrows HO_2^- + H^+ \quad pK_a = 11.6 \qquad (5)$$
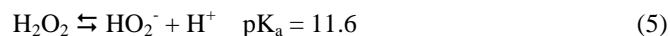
However, a high pH should be avoided because bicarbonate and carbonate ions (coming from the mineralization or present in the waters) are competitive $HO^\bullet$ trapping species.

In most degradations performed by UV/H_2O_2, optimum values for H_2O_2 concentration have been found, beyond which an inhibitory effect takes place [17]. At high H_2O_2 concentrations, competitive reactions occur in accordance with the following scheme [11]:

$$HO^\bullet + H_2O_2 \rightarrow HO_2^\bullet + H_2O \qquad (6)$$

$$HO_2^\bullet + H_2O_2 \rightarrow HO^\bullet + H_2O + O_2 \qquad (7)$$

$$2\ HO_2^\bullet \to H_2O_2 + O_2 \tag{8}$$

$$HO_2^\bullet + HO^\bullet \to H_2O + O_2 \tag{9}$$

Hydroxyperoxyl ($HO_2^\bullet$) radicals are produced through reaction (6), but these radicals are much less reactive than $HO^\bullet$ ($E^0 = 1.7$ *vs.* 2.8 V).

In all cases, it is necessary to determine the optimal H_2O_2 concentration, which will depend on the concentration and chemical nature of the pollutants in the effluent stream. Consequently, treatability tests are needed to determine the right amount of H_2O_2 and to validate the technology [11].

The use of UV/peroxide offers some advantages: the oxidant is commercially accessible, thermally stable, and can be stored in the site of use (with the required precautions). Since H_2O_2 has an infinite solubility in water, it is an effective source of $HO^\bullet$. There are no mass transfer problems associated with gases, as in the case of ozone. Since the needed amounts of the reagent are relatively low, the process is rather economical. The method has a low efficiency for treating waters of high absorbance at $\lambda < 300$ nm, or containing substances that compete with $HO^\bullet$ generation. In these cases, a large amount of H_2O_2 is needed [11].

The UV/H_2O_2 technology is one of the oldest AOPs and has been successfully used in the removal of contaminants from industrial effluents, including organochlorinated aliphatics, aromatics, phenols (chlorinated and substituted) and pesticides [5, 13]. It allows to extend the earlier UV-C technology for disinfection for simultaneous treatment of chemical detoxification.

At present, UV/H_2O_2 technology is totally commercialized. The method can be sensibly improved by combination with ultrasound or by pretreatment with ozone [11].

The kinetics of the UV/H_2O_2 process has been explained employing various types of kinetic models as shown in Table **2** [18,19]. The first category of kinetic models is a rate expression derived from an empirically determined correlation. Some experimental data from the oxidation of several compounds was successfully correlated using the power law model, including in some cases the effect of the UV intensity on the oxidation rate. The second type is a kinetic model based on reaction mechanism and known chemical and photochemical reactions.
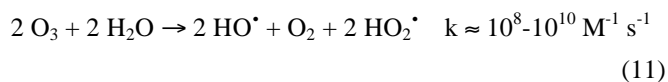
Recently [19], the decolorization of C.I. Acid Orange 7 (AO7) was investigated using the UV/H_2O_2 process in an annular continuous-flow photoreactor as a function of oxidant, dye concentrations, reactor length and volumetric flow rate. A design equation was used to predict the concentration of AO7 and the electrical energy per order (E_{EO}[2] [20]) at different conditions. Other authors [21] studied the photolytic degradation of AO7 by means of UV/H_2O_2 observing that the electrical energy needed for the mineralization process can be notably reduced by using the optimal H_2O_2 dosage.

A more ambitious approach was made by Alpert *et al.* [16] by using numerical models for the design and optimization of UV/H_2O_2 systems incorporating both reaction design (hydrodynamics, lamp orientation) and chemical kinetics (reaction mechanisms, kinetic rate constants) using computational fluid dynamics (CFD) and solving the fluid dynamics equations through space and time, including the conservation of mass, momentum, and energy. The authors concluded that effective CFD models for AOPs should incorporate rigorous turbulence and fluence rate submodels, kinetic rate equations, and proper characterization of the background water matrix. As soon as oxidation pathways for water contaminants are identified, a simulation model may become an important tool for the design and optimization of AOPs, and the model will allow evaluation of multiple design scenarios, including number of lamps, layout of reactors, and upstream hydraulic conditions. More advanced turbulence models, including those incorporating the Reynolds Stress Model and/or the Large Eddy Simulation, would enhance the modeling, together with a more rigorous method for validation of the UV fluence (dose) distribution in UV/AOP. In addition, reactors should be evaluated using multiple irradiance sensors and/or online chemical actinometers. Since the reaction mechanisms for additional emerging contaminants become available, especially quantification of specific byproduct formation, CFD should be considered as a tool for predicting the outcome of direct photolysis and advanced oxidation on environmentally important compounds.

2.2. UV/O_3

In the absence of light, ozone can react directly with an organic substrate, through a slow and selective reaction (eq. (10)) or through a fast and non-selective radical reaction producing $HO^\bullet$ (eq. (11)) [11]:

$$O_3 + S \to S_{ox} \qquad k \approx 1\text{-}100\ M^{-1}\ s^{-1} \tag{10}$$

$$2\ O_3 + 2\ H_2O \to 2\ HO^\bullet + O_2 + 2\ HO_2^\bullet \qquad k \approx 10^8\text{-}10^{10}\ M^{-1}\ s^{-1} \tag{11}$$

It has been demonstrated that ozone decomposition in aqueous solution forms $HO^\bullet$, especially when initiated by OH^- [11]:

$$O_3 + HO^- \to O_2 + HO_2^- \tag{12}$$

$$HO_2^- + O_3 \to O_3^{\bullet-} + HO_2^\bullet \tag{13}$$

$$HO_2^\bullet \leftrightarrows O_2^{\bullet-} + H^+ \tag{14}$$

$$O_2^{\bullet-} + O_3 \to O_3^{\bullet-} + O_2 \tag{15}$$

$$O_3^{\bullet-} + H^+ \leftrightarrows HO_3^\bullet \tag{16}$$

$$HO_3^\bullet \to HO^\bullet + O_2 \tag{17}$$

$$O_3 + HO^\bullet \leftrightarrows O_2 + HO_2^\bullet \tag{18}$$

The route can be initiated in different ways, by HO_2^-, $HCOO^-$, Fe^{2+}, humic substances or principally by HO^-. This is why, in principle, ozonation is sensibly more efficient in alkaline media, presenting an optimum around pH 9 [11].

It must be highlighted that ozone final products are O_2 and H_2O, making the method less toxic to other conventional treatments that use Cl_2 or chromic acid. Ozonation is a good pretreatment before a biological treatment, because complex organics are transformed into aldehydes, ketones or carboxylic acids, all easily biodegradable compounds. Ozonation is

---

[2] Electrical energy per order (E_{EO}) is the electrical energy in kilowatt hours (kWh) required to bring about the degradation of a contaminant C by one order of magnitude in 1 m^3 (1000 L) of contaminated water or air.

Table 2. Kinetic Rate Expression for Removal of Various Organic Compounds with the UV/H$_2$O$_2$ Process. Taken From [18,19 and References Therein]

Type of Kinetic Models	Organic Compound	Reactor Type	UV Source	Rate Equation
First category of kinetic models	Chlorophenols	Batch	Low-pressure Hg lamp	$-d[DOC]/dt = k_{H2O2}[DOC]^m [H_2O_2]^n + k_{UV} [DOC]_0 I^p + k_h [DOC]^q [H_2O_2]^r I^s$
	Benzene, toluene, phenol, methylphtalate	Batch	Low-pressure Hg lamp	$-d[DOC]/dt = k_{UV} [DOC]^m + k_h [DOC]_0 [H_2O_2]^n$
	Isoprene	Batch	Medium-pressure Hg lamp	$-d[DOC]/dt = k_{UV} [DOC]^m I^n + k_h [DOC]_0 [H_2O_2]^p I^q$
Second category of kinetic models	Acid Orange 7	Batch and continuous circulation	Low-pressure Hg lamp	$-d[DOC]/dt = 2 \phi f_{H2O2} k_h I [DOC] k_b^{-1} [DOC]_0^{-1}$ $f_{H2O2} = \varepsilon_{H2O2} [H_2O_2] (\varepsilon_{DOC} [DOC] + \varepsilon_{H2O2} [H_2O_2])^{-1}$
	Reactive Black 5	Recirculation	Medium-pressure Hg lamp	$-d[DOC]/dt = k_b I [H_2O_2] [DOC]\{(k_{b1} I + k_{b2}) [DOC]_0 + [H_2O_2])\}^{-1}$

m, n, o, p, q, r, s: reaction order.
k_b, k_{b1}, k_{b2}: constants used for the kinetic modeling.
k_h: reaction rate constant for UV/H$_2$O$_2$ system, min^{-1}.
k_{UV}: reaction rate constant for UV alone, min^{-1}.
ϕ: quantum yield.
ε: molar absorption coefficient M^{-1} cm^{-1}.
DOC: dissolved organic carbon.

also versatile to be combined with other conventional or AOPs.

However, from the operational point of view, there are limitations associated with the gas-liquid ozone mass transfer [11, 13]. Consequently, the process requires efficient reactor design in order to maximize the ozone mass transfer coefficient; increasing the interfacial area of contact (the bubble size by using small size diffusers, ceramic membranes, etc. [13]), good stirring, line mixers, contact towers, etc. can favor the process. In addition, increasing the retention time in the reactor by large bubble columns, or increasing the solubility of ozone by increasing the pressure to several atmospheres, may be effective.

Addition of H$_2$O$_2$ to the ozonation system enhances the oxidation capacity of the process through secondary reactions. Hydrogen peroxide initiates O$_3$ decomposition by electron transfer. Set of reactions (12) to (18) is initiated by HO$^\bullet$ producing reaction (19) [11]:

$$O_3 + H_2O_2 \rightarrow HO^\bullet + O_2 + HO_2^\bullet \qquad (19)$$
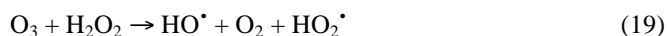
The process is expensive but fast, and can treat organic pollutants at very low concentrations (ppb), at pH between 7 and 8; the optimal O$_3$/H$_2$O$_2$ molar ratio is $\cong$ 2:1. It was suggested that the acceleration of ozonation is due to the increase of ozone transfer in water by H$_2$O$_2$.

One of the principal fields of application of this treatment is in the degradation of pesticides [6]. It is also effective for the post-treatment of water previously treated with chlorine because it can decompose trihalomethanes or related compounds.

When ozone is combined with UV irradiation, several processes take place. Irradiation of ozone in water leads to quantitative formation of H$_2$O$_2$ [22]:

$$O_3 + H_2O + h\nu \rightarrow H_2O_2 + O_2 \qquad (20)$$
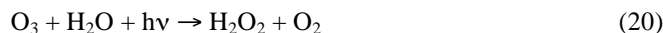
As said before, photolysis of H$_2$O$_2$ by UV-C radiation (see eq. (4)) yields two hydroxyl radicals per each molecule of hydrogen peroxide; the reagent also reacts with O$_3$:

$$H_2O_2 + h\nu \rightarrow 2 HO^\bullet \qquad (4)$$

$$O_3 + H_2O_2 \rightarrow HO_2^\bullet + HO^\bullet + O_2 \qquad (21)$$
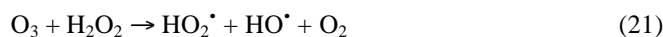
As well as H$_2$O$_2$ (eq. (6)), ozone reacts with hydroxyl radicals to form superoxide radicals:

$$O_3 + HO^\bullet \rightarrow O_2 + HO_2^\bullet \qquad (22)$$

Since ozone has a higher absorption coefficient than H$_2$O$_2$ ($\varepsilon_{254} = 3300$ M^{-1} cm^{-1}), this combined AOP can be used to treat water with high UV absorption background [11]. The efficiency is higher than that of O$_3$ or direct UV, because UV-B light (280-315 nm) can be used, avoiding the use of a quartz reactor.

When UV-C irradiation is used, photolysis of O$_3$ generates additional HO$^\bullet$ and other oxidants, with the subsequent increase of the efficiency [11]:

$$O_3 + h\nu \rightarrow O_2(^1\Delta g) + O(^1D) \qquad (23)$$

$$O(^1D) + H_2O \rightarrow 2 HO^\bullet \qquad (24)$$

The Heliozon process combines solar light with ozonation, producing a noticeable increase of the reaction rate of ozone activation as proved in the degradation of phenol and malic acid [23]. This brings a possible way to increase ozone reactivity at a low cost.

2.3. Photo-Fenton and Related Processes

In acid solution and in the dark, the decomposition of H_2O_2 catalyzed by Fe^{2+} in solution leads to the production of hydroxyl radicals, according to the well known thermal Fenton reaction [6]:

$$Fe^{2+} + H_2O_2 \rightarrow Fe^{3+} + HO^- + HO^{\bullet} \quad k = 76 \text{ M}^{-1} \text{ s}^{-1} \text{ [24]} \quad (25)$$

In the presence of H_2O_2 and at pH < 3, the reaction system is autocatalytic, because Fe^{3+} decomposes H_2O_2 into O_2 and H_2O through a chain mechanism [24]:

$$Fe(III) + H_2O_2 \rightarrow Fe(II) + H^+ + HO^{\bullet} \quad k = 0.01\text{-}0.02 \text{ M}^{-1} \text{ s}^{-1} \tag{26}$$
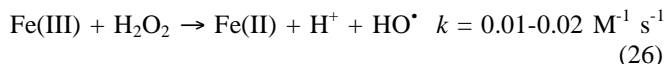
The optimum pH value commonly used in the Fenton reaction is determined in order to avoid the precipitation of iron species that would interfere in the reaction; besides, an additional elimination step should be introduced in the treatment with the consequent extra cost. As can be seen in equation (26), the process can be initiated by Fe^{3+}, but the reaction would be slower because Fe^{2+} must be formed first. Copper(II) can be used in place of iron.

When a Fenton system is irradiated with ultraviolet light, reaction rates are highly improved in most of the cases because several processes contribute to the increase of the $HO^{\bullet}$ formation rate:

a)   UV photolysis of Fe^{3+} hydroxocomplexes. This process, in spite of a low quantum yield of $HO^{\bullet}$ formation, will promote the photochemical reduction to Fe^{2+} :

$$Fe(OH)^{2+} + h\nu \rightarrow Fe^{2+} + HO^{\bullet} \tag{27}$$
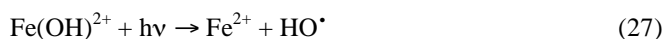
b)   When there are ligands (L) present in solution that could form photochemically active Fe(III) complexes under excitation by UV-Vis irradiation (like iron complexes with some carboxylic acids), ligand to metal charge transfer (LMCT) reactions take place yielding Fe(II) and products of oxidation of the ligand (L_{ox}); in the case of oligocarboxylic acids (*e.g.*, oxalic acid), these reactions proceed with high quantum yields (eq. (28)):

$$Fe^{3+}\text{-}(L)_n + h\nu \rightarrow Fe^{2+}\text{-}(L)_{n-1} + L_{ox} \tag{28}$$
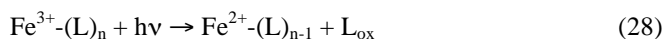
c)   Depending on the used irradiation wavelength and the photoproperties of the target compound, direct photolysis can take place.

d)   If light of wavelengths lower than 300 nm are employed, UV photolysis of H_2O_2 takes place, leading to additional $HO^{\bullet}$.

Fig. (**1**) is a scheme of all the possible pathways involved in the photo-Fenton process.

The overall rate of the photo-Fenton process is controlled by the rate of the photolytic step that converts Fe^{3+} back to Fe^{2+}, and the continuous Fe(II)/Fe(III) recycle makes the process autocatalytic.

The most frequent use of the photo-Fenton process has been the treatment of industrial waters and lixiviates. Nitroaromatics, polychlorinated phenols, herbicides (2,4,5-trichlorophenoxyacetic (2,4,5-T), 2,4-dichlorophenoxyacetic acid (2,4-D)) and other pesticides have been successfully degraded [11].

Photo-Fenton processes can use sunlight instead of UV light with a minor decrease in the rate of degradation. According to Gogate and Pandit [14], this is a very important factor for the scale-up and commercial use of a PAOP, since the costs of treatments will be substantially lowered if sunlight is used. The photo-Fenton process can take advantage of the presence of constituents of real effluents like iron or copper salts, avoiding an additional dosage, and oligocarboxylic acids such as oxalate or ethylenediaminetetraacetic acid (EDTA), which form photochemically active iron(III) complexes and enhance the process. Appropriate selection of the iron salts needs to be done, and use of oxalate ions as the counter-ions is recommended for the majority of the pollutants and reaction conditions [14].

The role of iron on the degradation of different organic compounds, differing in their structure (aliphatic versus aromatic) and iron complex formation capacity, by conventional and photo-Fenton processes was recently investigated by Hermosilla *et al.* [26]. It has been seen that these chemical characteristics can affect the degree of treatment in terms of COD (chemical oxygen demand) and TOC (total organic carbon) removals. While aromatics exhibited a fast and pronounced reduction in the COD by conventional Fenton process, aliphatic compounds required the presence of UV light to enhance treatment results.
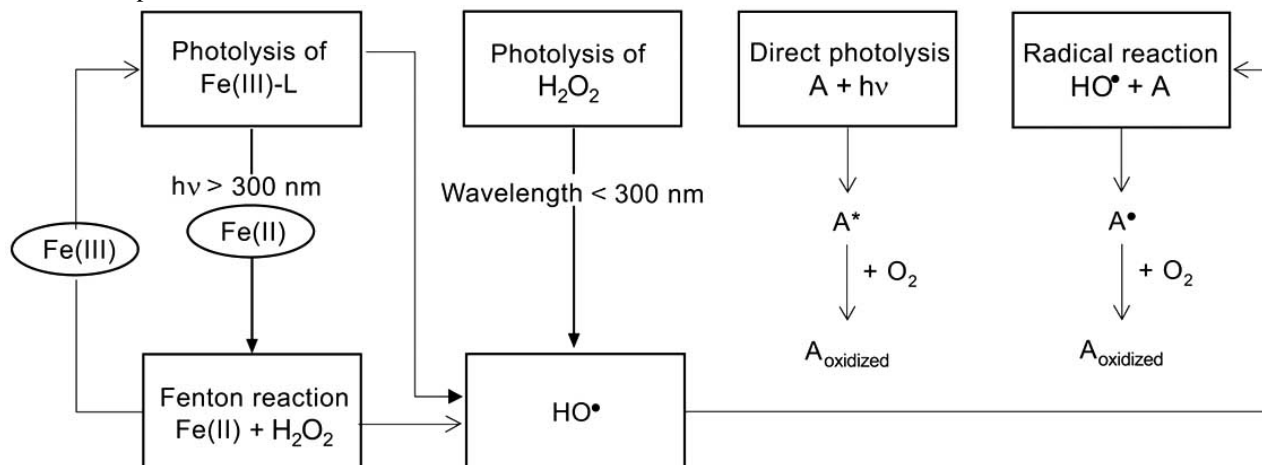

Fig. (1). Scheme of chemical reactions in the photo-Fenton reaction (adapted from reference [25]).

Many publications can be found in the literature on applications of Fenton and photo-Fenton processes and the revision will not be done in this article.

2.4. Heterogeneous Photocatalysis

Heterogeneous photocatalysis is a very well known technology, valuable for purification and remediation of water and air. Several excellent revisions exist on the subject, with different approaches (see for example [5, 7-10,13,27-29]).

In HP, after excitation of a semiconductor with light of energy equal to or higher than the bandgap (E_g), conduction band electrons (e_{cb}^-) and valence band holes (h_{vb}^+) are created. TiO_2 is so far the most useful semiconductor material for photocatalytic purposes, owing to its exceptional optical and electronic properties, chemical stability, non-toxicity and low cost. The energy bandgaps of the photocatalytic forms of TiO_2, anatase and rutile, are 3.23 eV (corresponding to 384 nm) and 3.02 eV (corresponding to 411 nm). The most popular and photoactive commercial form of TiO_2 is produced by the German company Degussa (now Evonik) under the name P-25. For Degussa P-25, the values of the edges of conduction and valence bands at pH 0 have been calculated as -0.3 and +2.9 V, respectively [30]. Photogenerated holes and electrons can recombine easily (this being one of the most important drawbacks of the process for its application) or migrate to the surface where they can react with donor (D) or acceptor (A) species (Fig. **2**).
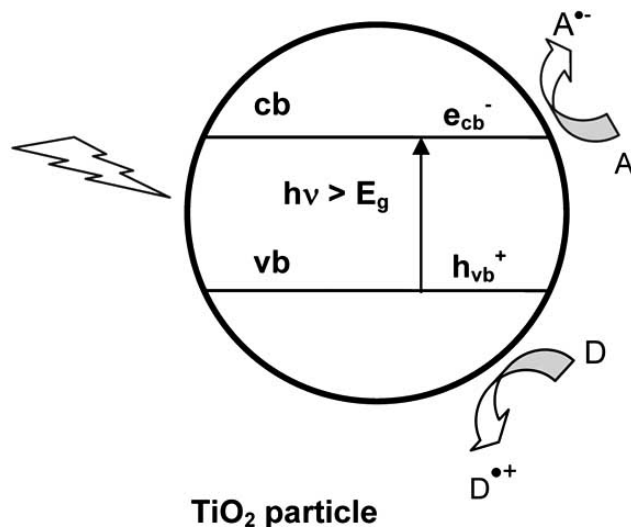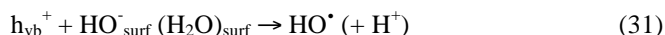

Fig. (2). Simplified diagram of the heterogeneous photocatalytic processes occurring at an illuminated TiO_2 particle.

The energy level at the bottom of the conduction band is actually the reduction potential of photoelectrons and the energy level at the top of the valence band determines the oxidizing ability of photoholes, each value reflecting the ability of the system to promote reductions and oxidations. Valence band holes are strong oxidants that may attack directly oxidizable species D or form HO$^\bullet$ from water or surface hydroxide ions, while conduction band electrons are mild reducing acceptors. From a thermodynamic point of view, the couples present in the system can be photocatalyti-

cally reduced by conduction band electrons if they have redox potentials more positive than the flatband potential[3] (V_{fb}) of the conduction band, and can be oxidized by valence band holes if they have redox potentials more negative than the V_{fb} of the valence band [12 and references therein].

The above-described scheme is completed by the following basic equations where e_{cb}^-, h_{vb}^+ and HO$^\bullet$ are involved:

$$TiO_2 + h\nu \rightarrow e_{cb}^- + h_{vb}^+ \qquad (29)$$

$$e_{cb}^- + A_{\,surf} \rightarrow A^{\bullet-} \qquad (30)$$

$$h_{vb}^+ + HO^-_{\,surf}\,(H_2O)_{surf} \rightarrow HO^\bullet\,(+\,H^+) \qquad (31)$$

$$h_{vb}^+ + D_{\,surf} \rightarrow D^{\bullet+} \qquad (32)$$

where *surf* indicates that the species are adsorbed or close to the TiO_2 surface.

Titanium dioxide is an excellent photocatalytic material useful for environmental applications [8]. Depending on the exact conditions, holes, HO$^\bullet$, and $O_2^{\bullet-}$ radicals, H_2O_2 and O_2 will play a very important role in the photocatalytic mechanisms.

Donor oxidation can also occur by attack of HO$^\bullet$, following eqs. (1)-(3):

$$HO^\bullet + D \rightarrow D^{\bullet+} \qquad (33)$$

It is important to note that in addition of oxidizing organic compounds as proposed in section 2.1, HP can transform also toxic metal ions [9,10,12] and even destroy microbiological contamination (see for example reference [31]).

In some cases, addition of a noble metal to the TiO_2 surface increases the photocatalytic activity, although the activity of the transformed photocatalyst depends largely on the target pollutant [27,32].

Solution pH affects HP due to its influence on the superficial electric charge on the semiconductor (influencing the redox level of the charge carriers, i.e., electron and holes), the speciation of compounds in solution, and the values of their redox potentials. The pH affects the position of the flatband, which is reduced in 59 mV with every pH unit, according to the following equation [33]:

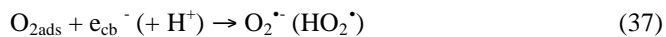$$E_{fb}(pH) = E_{fb}(pH_0) - 0.059\ pH \qquad (34)$$

The point of zero charge (pH_{pzc}), i.e. the pH value in which the catalyst superficial charge is zero, is around 6.5 in the case of TiO_2. Above and below the pH_{pzc}, the catalyst surface is negative or positive, according to the following protolytic equilibria:

$$TiOH_2^+ \leftrightarrows TiOH + H^+ \qquad (35)$$

$$TiOH \leftrightarrows TiO^- + H^+ \qquad (36)$$

The hydroxyl anions act as receptors of the photogenerated holes and are very important for the semiconductor photocatalytic activity because they produce HO$^\bullet$ (eq. (31)). In addition, the superficial sites with high acidity favor, in some cases, the adsorption, and are better h_{vb}^+ traps.

---

[3] The flat band potential (V_{fb}) is defined as the potential of the semiconductor at which there is no excess of charge, no electric field and no space charge region.

The addition of an oxidant to the system inhibits recombination of electrons and holes and the photocatalytic system can become more efficient. For example, in aerated suspensions, O_2 is adsorbed onto the TiO_2 surface, acting as an electron acceptor and leading to the formation of superoxide anions (eq. (37)) in a thermodynamically feasible but rather slow electron transfer reaction. Values of $E^0(O_2/O_2^{\bullet-})$ = -0.3 V and $E^0(O_2/HO_2^{\bullet})$ = -0.05 V have been reported for homogeneous solutions; the reduction potentials onto the TiO_2 surface are probably less negative. As the following set of equations indicates, this cathodic pathway is an additional source of hydroxyl radicals and hydrogen peroxide is produced.

$$O_{2ads} + e_{cb}^- (+ H^+) \rightarrow O_2^{\bullet-} (HO_2^{\bullet}) \tag{37}$$

$$O_2^{\bullet-} + H_2O \rightarrow HO_2^{\bullet} + OH^- \qquad pK_a = 4.8 \tag{38}$$

$$2\ HO_2^{\bullet} \rightarrow O_2 + H_2O_2 \tag{8}$$

$HO_2^{\bullet}/O_2^{\bullet-}$ radicals are not very reactive for attacking organic compounds but their electron transfer reactions can be very fast.

Another important oxidant is H_2O_2. Besides the amount formed by eq. (8), external dosage of hydrogen peroxide to a HP system contributes to the formation of additional hydroxyl radicals, as well as trapping of conduction band electrons (eq. (39)) or reaction with superoxide radicals (eq. (40)), especially at high H_2O_2 concentrations [9].

$$H_2O_2 + e_{cb}^- \rightarrow HO^- + HO^{\bullet} \tag{39}$$

$$H_2O_2 + O_2^{\bullet-} \rightarrow HO^- + HO^{\bullet} + O_2 \tag{40}$$
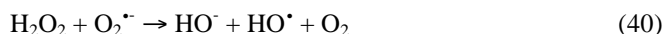
However, as already said, H_2O_2 is a $HO^{\bullet}$ scavenger (see eqs. (6) to (9)).

Dissolved transition metals M^{n+}, like Fe^{3+}, increase the rate of the photocatalytic oxidation of organic compounds due to the reduction of the metallic ion by conduction band electrons (eq. (41)), which inhibits the deleterious electron-hole recombination [9]:

$$M^{n+} + e_{cb}^- \rightarrow M^{(n-1)+} \tag{41}$$

In this case, due to H_2O_2 production (eq. (8)), photo-Fenton reactions also take place, enhancing $HO^{\bullet}$ production and increasing the oxidizing power of the process.

An additional serious limitation for TiO_2 technological applications is the requirement of UV light to promote chemical processes due to the wide semiconductor bandgap. Attempts to extend the range of activity of TiO_2 to the visible have been made in various ways: (a) ion implantation, (b) use of coupled semiconductors like TiO_2-CdS or ZnO-CdS photocatalysts; (c) substitution of non-metals like N, C, S, P or B for oxygen sites in the TiO_2 lattice; (d) attachment of suitable dyes [34 and references therein]. However, all these techniques present several drawbacks and the photoactivity of these modified semiconductors is still rather low for real application.
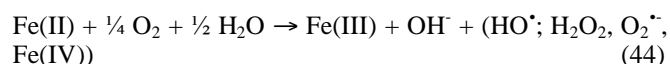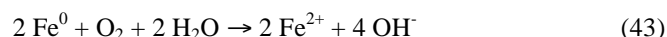
2.5. Zerovalent Iron (ZVI)

Zerovalent iron is an emergent material, increasingly used for the treatment of several pollutants, particularly chlorinated organics, nitroaromatics, nitrate, azo-dyes, toxic metal ions and arsenic in solution [35-37]. The technology is

based on the use of iron in the elemental state and the material can be employed in various forms: microparticles (powders), fillings, wires, nails, wool and, in recent times, nanoparticles. The physicochemical processes taking place in this technology depend on pH, the nature of the pollutant and other factors. In some cases, a reducing process takes place but, depending on the conditions, the process is oxidative [36]. In water and in the absence of oxygen, reductive Fe^0 corrosion takes place:

$$Fe^0 + 2\ H_2O \rightarrow Fe^{2+} + H_2 + 2\ OH^- \tag{42}$$
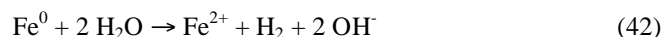
This process is increasingly used to remediate profound, reducing groundwaters, by means of reactive permeable barriers containing zerovalent iron. Several pollutants (chlorinated aliphatics, Cr(VI), etc.) could be satisfactory reduced by the method, but the mechanisms are not totally clear so far [38].

In H_2O and under O_2, oxidative Fe^0 corrosion leads to formation of Fe(II), Fe(III) and ROS; reaction of Fe(II) with H_2O_2 ends in the Fenton reaction, with $HO^{\bullet}$ production. Fresh iron oxyhydroxides (FHO: iron rusts, magnetite, lepidocrocite, maghemite) precipitate as flocs with a continuous Fe(II)/Fe(III) cycle.

$$2\ Fe^0 + O_2 + 2\ H_2O \rightarrow 2\ Fe^{2+} + 4\ OH^- \tag{43}$$

$$Fe(II) + \tfrac{1}{4}\ O_2 + \tfrac{1}{2}\ H_2O \rightarrow Fe(III) + OH^- + (HO^{\bullet};\ H_2O_2,\ O_2^{\bullet-}, Fe(IV)) \tag{44}$$

$$Fe^{2+} + H_2O_2 \rightarrow Fe^{3+} + HO^- + HO^{\bullet} \tag{26}$$

$$Fe\ (II)/(III) + 3\ H_2O + O_2 \rightarrow FHO\ (flocs) \tag{45}$$

The intermediates formed during ZVI corrosion can oxidize species (e.g. As(III) to As(V)), and fresh FHO are strong adsorbents of metal and metalloid species. Therefore, in these cases, removal by ZVI takes place mainly by adsorption and coprecipitation onto these FHO flocs.

ZVI has several advantages compared to other materials: (i) it is cheap and widely available in many forms, (ii) it is simple and can be easily handled, (iii) the technology can be straightforwardly scalable, (iv) it can be improved by solar light.

ZVI reactions are rather slow, but the process can be notably accelerated using iron nanoparticles (NZVI) [36 and references therein]. The tiny particle size, the large surface area and the high density of reactive surface sites (or surface sites of high intrinsic reactivity) lead to a very high efficiency, and make these materials very attractive for remediation.

The effect of UV or H_2O_2 addition on the ZVI technology, involving Fenton-type processes, has been addressed [36 and references therein]. Studies on UV irradiation, economically promissory because solar light can be used, were generally focused on As(III) oxidation. The solar ZVI technology was used to modify the SORAS technology (Solar Oxidation and Removal of Arsenic) [39]. SORAS removes arsenic from water in polyethyleneterephtalate (PET) bottles by photo-Fenton processes taking place by addition of lemon juice (citrate) and solar light, for example in natural waters of Bangladesh. The method was modified for waters not containing enough amounts of natural iron and with considerable amounts of natural organic matter (NOM) by addition

of ZVI (wires, wool, nanoparticles). In this case, PF processes take place by iron corrosion followed by reaction of iron in solution with NOM. As(III) photooxidation at low pH in the presence of oxygen was studied for application in the remediation of acid mine waters [40].

3. PRACTICAL APPLICATIONS

3.1. Coupling of AOPs with Biological Treatments

The use of AOPs as a single treatment stage is not economically convenient to treat large volumes of effluents due to high electrical or chemical costs compared with biological treatments. On the contrary, although biological treatments are cheaper, they are time-consuming and several pollutants are biorecalcitrant. In last times, some studies aimed to reduce the toxicity of an effluent with an AOP up to a certain level beyond which a biological oxidation is applied to achieve total detoxification; the application of the initial AOP pretreatment decreases the total treatment time. Due to the extension of this article, these couplings will not be described here, but several references can be found in the literature [41-43].

3.2. Comparative Studies on AOPs

The election of one AOP for the treatment of a wastewater must be evaluated from an economical and practical point of view. Mostly, the choice of the AOP is based on its effectiveness to achieve the target concentration, pH, COD, etc. and, once the process is shown to be adequate, the election must be economical. The criteria to compare the performance depend highly on the properties of the wastewater.

From the existing literature, it can be seen that generally direct photolysis results in incomplete and slow degradation of the pollutant unless the target compound absorbs strongly at the irradiation wavelength. Addition of H_2O_2 to the UV illuminated system results in a faster degradation; however, a strict control of the H_2O_2 dose is needed to avoid excess of the reagent, which becomes a competitor for $HO^{\bullet}$ according to reactions (6) to (9)). It has been observed, when comparing different technologies, that photo-Fenton is generally the most efficient, and complete mineralization occurs in most cases only using the individual process; however, the ratio of reagents (i.e., the Fe/H_2O_2 molar ratio) needs to be always optimized. Another drawback of the PF technology is that acid pH is needed and must be maintained to prevent precipitation of iron compounds. This restriction adds a previous acidification step and the further alkalinization for iron elimination of the media [44].

Gogate and Pandit [13] compare five different oxidation processes: cavitation, HP, Fenton processes, ozonation and use of H_2O_2. Although US/cavitation is not treated in the present article, the reference should be consulted as the following main points highlighted by the authors are applicable to all AOPs:

1) The efficacy of the process depends strongly on the rate of generation of free radicals together with a good contact of these radicals and/or chemical oxidants with the pollutant molecules; the efficient design should then aim at maximizing both features.

2) Although a large amount of literature is available for application of HP to wastewater treatment for different model pollutants, studies with real effluents are scarce and strong efforts are required in this direction.

3) The development of global kinetic models to predict the reaction rates, helpful in designing large-scale reactors, are needed. The models should be function of critical parameters such as pollutant concentration, presence of radical scavengers, or presence of constituents enhancing the rates by arresting the electron-hole recombination.

4) Fenton chemistry seems to be beneficial if used as a supplement to enhance the rates of, e.g., HP and acoustic cavitation processes rather than its use as individual technology.

5) Ozone or hydrogen peroxide as individual processes are not economically favorable, and they should be used in combination with others (mainly ultrasound and UV irradiation, which lead to the formation of free radicals).

3.3. Combination of AOPs

Although most AOPs can be used individually in wastewater treatment applications with good economics and high degree of energy efficiency, hybrid methods (mostly a combination of AOPs) generally improve the global treatment. These combinations increase the photoprocess efficiency by decreasing the reaction time in respect to the separated operations, or decrease the cost in respect of HP alone, generally in terms of light energy. The most used combinations are $UV/O_3/H_2O_2$, photo-Fenton processes combined with TiO_2, combinations with PAOPs with ultrasound, wet air oxidation or other non-photochemical AOP, etc. As said before, combination of AOPs with conventional methods, mainly biological oxidation, is very much studied at present. The choice of the combination will be dictated by the type of wastewater to be treated. It is always mandatory to perform a treatability study of wastewaters before real application of the technologies.

Recently, Lucas *et al.* [45] compared different ozone-based advanced oxidation processes (O_3, O_3/UV and $O_3/UV/H_2O_2$) for the treatment of winery wastewater in a pilot-scale bubble column reactor. It was found that at the natural pH of the studied wastewater (pH 4), $O_3/UV/H_2O_2$ was the most effective treatment, followed by O_3/UV and O_3. The authors performed an economic analysis of the operating costs showing that the $O_3/UV/H_2O_2$ combination was also the most economical process (1.31 Euro m^{-3} g^{-1} of TOC mineralized under optimized conditions).

A recent review [22] analyzes combinations of HP with chemical and physical operations as tools for improving the photoprocess performance. In the specific case of HP, two categories of combinations were considered because the efficiency may be affected by different factors. In the first one, the technology influences directly (and can enhance) the photocatalytic mechanism, as this is the case of e.g. ultrasonic irradiation, photo-Fenton, ozonation or electrochemical treatments. A second category includes the coupling with methods not affecting the photocatalytic mechanism, such as biotreatments, membrane reactor, membrane photoreactor, or

physical; in these cases, the combination increases the efficiency of the overall process. Thus, the application of the combined technologies should be directed to the factors affecting these two different aspects. The authors highlight that the main drawback of HP are the very low quantum efficiencies reached ($< 1\%$), which implies that only one over one hundred of the incident photons is able to produce an oxidation/reduction step. Depending on the concentration of the contaminant present and on the desired degree of oxidation, it is necessary to provide the photoreacting system with a photon flow two orders of magnitude higher than that eventually utilized. In real contaminated waters, having different pollutants, at high concentrations and in high volumes, the magnitude of the photon flow needed for the treatment would be very high, and the process would not be economic. Sun can also give photons but only ca. 5% of them (ca. 30 W m^{-2}) can be used by TiO_2 (due to its bandgap), and this cannot satisfy the needs of the treatment in a realistic way. Based on these considerations, the authors propose that the use of photocatalysis for wastewater remediation would be successful if addressed only to the transformation of recalcitrant to non-recalcitrant compounds, which subsequently can be easily degraded by conventional techniques. Therefore, the coupling of HP with other chemical and physical operations seems a good strategy to achieve the remediation goal. Additionally, for each system, treatability tests in different conditions must be done to find the best technology.

Gogate and Pandit [14] detailed a series of important observations and recommendations for the use of combined AOPs. This corresponds to the first category of combinations cited in the above paragraph: the synergism is mainly due to generation and attack of $HO^{\bullet}$, *i.e.* both methods influence the controlling reaction mechanism, resulting in higher oxidation rates. Again, as stated in section 3.2, this reference should be consulted because all the observations of the authors are relevant for the general combination of AOTs and should be taken into account. The authors cite combination of ultrasound (not treated here) with O_3 or H_2O_2, claiming that the process produces enhanced dissociation of the reagents and then, higher degradation rates. In addition, the higher turbulence generated by ultrasound decreases the mass transfer resistance, a major limiting factor for the application of the individual reagents. On the other hand, combination of UV irradiation with O_3 and/or H_2O_2 is beneficial only when radical attack is the controlling mechanism and when some of the constituents of the effluent are refractory to the individual methods or require higher degree of oxidation. Dosage and ratio of reagents together with operating pH should be optimized. As always, the reactor design is another crucial factor.

An extensive study on the degradation of various carboxylic acids, oxalic acid [46], citric acid [47], gallic acid (Gal) [48] and EDTA [49-51] has been performed combining HP and PF, and this study shed light to the influence of the composition of the effluent in the PAOP treatment. For all the studied compounds, the formation of Fe(III)-L type complexes resulted very important due to the possibility of LMCT photolytic reactions under UV radiation. However, the different Fe(III)-L react with different quantum yields, leading to different efficiencies in the photocatalytic systems. In some conditions, the homogeneous processes were

very efficient and TiO_2 acted just as a screen, reducing the efficiency of the homogeneous reaction (this is the case of oxalic acid, whose Fe(III) complex photolyzes with very high quantum yield). Gallic acid showed very distinctive results due to the instability of the Fe(III)–Gal complex that undergoes homogeneous thermal charge transfer reactions strongly dependent on the molar ratio between Fe and Gal but without producing mineralization. Nevertheless, it was found that, even when high percentages of Gal conversion can be achieved in Fenton systems, UV irradiation is necessary in order to mineralize the aliphatic compounds produced after the thermal degradation of Gal.

4. RECENT PATENTS ON AOP SYSTEMS

As said before, in spite of the big amount of published scientific papers, not a large quantity of applications and/or patented work can be found related to photochemical AOPs. Most of them rely on one of the biggest problems when using photocatalytic techniques for water purification or treatment, which is the necessity of fixing the photocatalyst to a convenient support to avoid a further costly separation.

In the case of HP using TiO_2 in suspension, elimination and/or recovery of the photocatalyst leads necessarily to additional costs [52]. On the other hand, immobilized semiconductors do not offer the same efficiency than slurries, due to mass transfer limitations, mechanical stability and low profit of the incident light; therefore, in last years, many efforts have been made to improve the efficiency of supported catalysts.

A similar problem appears with the homogeneous photo-Fenton reaction: in last times, it was observed that the use of immobilized iron was advantageous because: 1) this leads to a synergy as the pollutant gets closer to the vicinity of the photocatalyst, with an additional stability (see section 4.2); 2) the immobilization allows to extend the operative pH range in comparison to that of the homogeneous system (higher working pH can be used).

In what follows, recent patents (since 2003) will be briefly reviewed. It is important to mention that earlier relevant works can be found in the literature and that the present study is not completely exhaustive.

4.1. HP Related Patents

4.1.1. System for Photocatalytic Treatment Using TiO₂ as Slurry (US7008473B2)

A photocatalytic process using TiO_2 as slurry was proposed to treat aqueous wastes [53]. The most relevant feature of the system is that it includes a converter (a gas scrubber) used to transfer gaseous contaminants into the aqueous photocatalytic slurry that, in addition to contaminated waters, allows treating other varying types of media, including air, soil or adsorbents (for example, activated carbon). Fig. (**3**) is a diagram of the system (1) used to transfer gaseous contaminants into the aqueous phase. A contaminated gas stream such as air having airborne contaminants is transferred by pipe (2) into a gas scrubber tower (3) where the pollutants are converted or transferred to the aqueous phase. At the top of the tower, a nozzle (4) disperses a solvent or the photocatalytic slurry into the tower. The atomized mole-
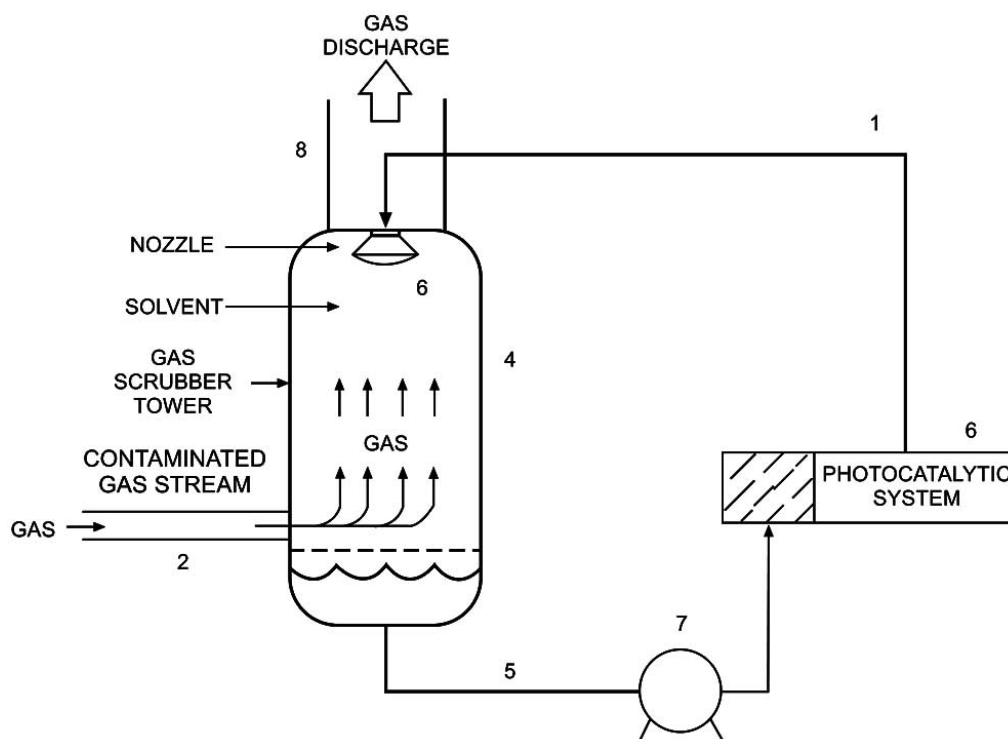
Fig. (3). Scheme of a photocatalytic system (**1**) for treatment of air, soil or aqueous contaminants by transference to a liquid phase (adapted from [53]).

cules of the liquid may be passed to the tower through lines (5) by a pump. The contaminated air stream encounters the downward moving solvent in the scrubber and the pollutants are then transferred to the aqueous phase by adsorption or absorption, downward to the bottom of the tower. Then, they are directed to the photocatalytic system (6) by pump (7), where they are treated. Gas free of pollutants is discharged through gas discharge (8).

In the case of the airborne contaminants, the process includes the following steps:

1) Removal of contaminants from the contaminated media using water or another solvent.

2) Oxidization and/or reduction of contaminants dissolved in the solvent, by mixing in a TiO_2 slurry and exposing to UV irradiation. Other oxidants can be added (such as H_2O_2).

3) Removal of the oxidation by-products from solvent, for example, by distillation, RO, etc.

4) Reuse of the solvent.

The invention provides the technical advantage of increasing the mass transfer of the air phase organic contaminant and the photocatalyst. In addition, the scaling-up of the reactor can be easily accomplished by increasing the number and size of nozzles for air injection and the size of the reaction chamber. Air treatment systems can be implemented to treat volumes of air of up to hundreds of thousands of cubic feet per minute. The system could be safely used to treat explosives (for example, nitroglycerine) or flammable contaminants in the aqueous phase rather than in the air phase.

4.1.2. Three Dimensionally Reticulated Open Cell Composed of Supported Semiconductor (US6524447B1)

An interesting patent [54] claims to offer an effective, quantum efficient, durable, economic, commercial apparatus for rapid HP purification and disinfection of water and ultrapure water, achieving a reduction of the organic charge to 500 ppt (parts-per-trillion) in TOC. In the system, polluted water is directed through a semiconductor unit, where a photocatalyst removes the contaminants. This unit is an open cell, three dimensionally reticulated, fluid permeable, composed of a rigid substrate (alumina, titania, silica, glass, quartz or organic polymers) integrated with a semiconductor (TiO_2, ZnO, $CaTiO_3$, etc.). The creation of turbulence by the device is an enhancement of the invention. A light emitting device in optical proximity with the semiconductor unit allows optimizing mass transfer, surface area, illumination, water flow, durability, rigidity, etc. A metal like Pt or similar can be incorporated to enhance the photocatalytic efficiency. Lamps to be used can emit from the UV to the visible range. Fig. (**4**) shows an example of a point of use reactor (9) with light-emitting diodes (LEDs) as the source of irradiation.

The water flows into the reactor through inlet (10) and then through the reticulated semiconductor unit (11), photoactivated by LEDs (12), hold by a support/wiring plate (13). A quartz plate (14) is provided to isolate the LEDs from the water flow. Purified water exits the reactor through outlet (15). Enclosure (16) can be constructed from a variety of materials resistant to LED light and to corrosion by water, such as thermoplastics (polypropylene, etc.) or metals (stainless steel). The reactor was designed for commercialization into markets defined by low and intermittent demand for purified water, such as household drinking water. The sys-
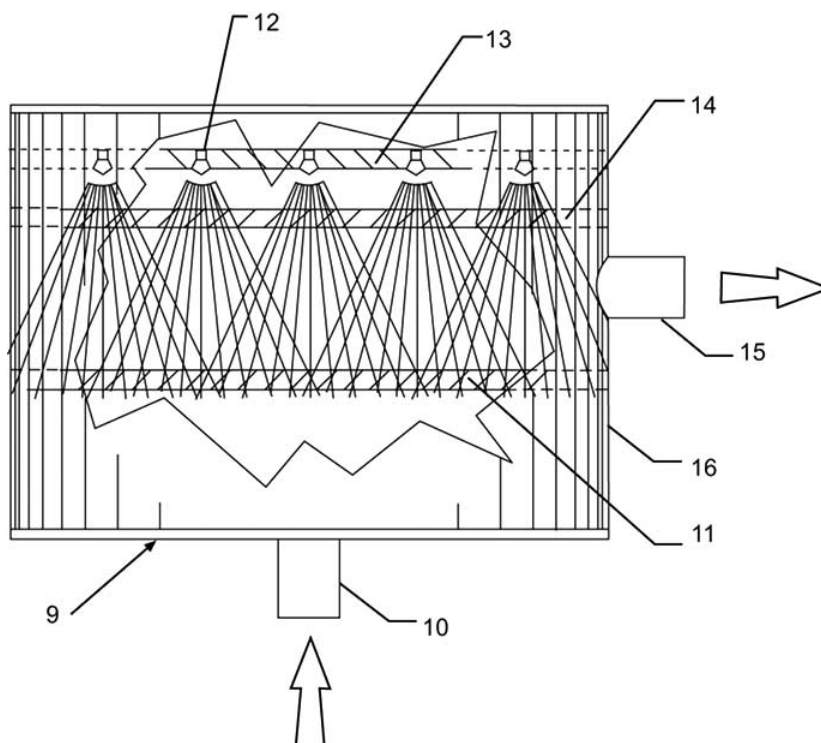
Fig. (4). Point of use photoreactor using LEDs as the irradiation source (adapted from [54]).

tem only requires low power electrical energy per LED, making it both safe for the user in an environment that includes water and electricity, and enabling the reactor to be utilized in portable applications (battery powered).

In the same invention [54], a commercial/industrial reactor (17) with tube type lamps as light sources is presented. The reactor is constituted by a cylindrical tube (18) where the water flows in and passes radially through the reticulated photocatalytic substrate and axially past the UV light source (Fig. **5**). Both the inner (19A) and outer light (19B) tubes are enclosed by cylindrical quartz sleeves. The contaminated water flows radially through the reticulated semiconductor unit and passes by the exterior lights. Purified water exits through outlet (20). The configuration of the reactor is designed to be modular so that longer and/or parallel reactors can be employed for higher flows. This reactor is designed for commercialization into markets defined by high and continuous demand for purified water.

4.1.3. Photocatalytic Membranes (EP1555064A1)

The application of photocatalytic membrane reactors (PMRs) appears as a promising method for solving problems concerning separation of the photocatalyst [55]. Invention [56] presents the use of microporous photocatalytic membranes (0.2 to 10 μm) suitable for the photochemical degradation and transformation of organic and inorganic pollutants. The membrane contains a semiconductor (TiO_2, ZnO), a photopromoter and a photosensitizer supported by photografting on the surface of a microporous support. The support can be a metal, whose surface is oxidized by different known techniques, or made on glass, ceramic or polymer, either in compact or in fiber form. The photografted layers afford a continuous permeability through the microporous membrane, increasing the reactivity compared with other membranes [57], and they do not show any problems connected to degradation of polymeric components, being resistant to UV irradiation.

The semiconductor nanopowder (25-250 nm thick) was deposited first by chemical vapor deposition or plasma tech-
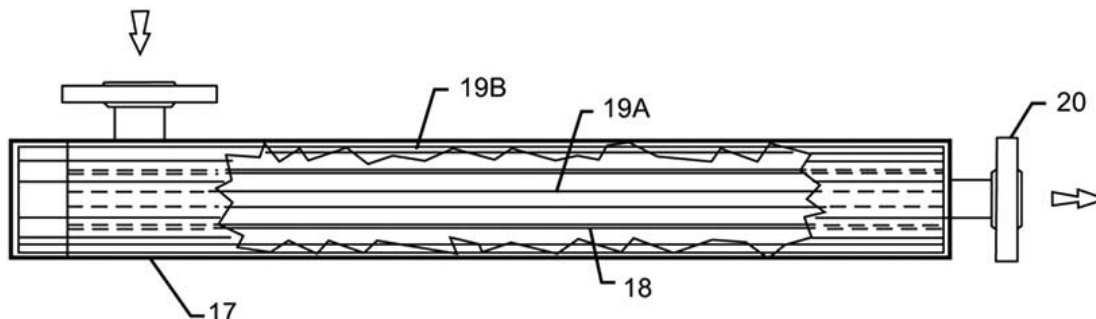

Fig. (5). Detail of a cylindrical reactor where the water flows in and passes radially through a reticulated photocatalytic substrate (adapted from [54]).

niques on the support. A second layer (250 nm-100 μm) was formed spraying or depositing an organic solvent suspension containing a semiconductor, a photoinitiator (an organometallic compound), a photosensitizer (a dye) and a photopromoter (a peroxometallic compound, triethylvanadate, iron(III) potassium oxalate, etc.). The photopromoter and the photosensitizer can be the same substance and this allows to extend the photocatalytic activity to the visible range and to increase up to 30-40 times the photocatalytic efficiency. This layer is irradiated by UV for curing, with the objective of exploiting the antenna effect of photopromoters. Thus, different photoreactor geometries and configurations could be modeled choosing the adequate membrane geometry: plane, tubular, hollow fibers.

A particular test at laboratory scale was performed to assess photodegradation of chloroaliphatics. Disc membranes (6 cm diameter), immobilizing only 25-35 wt% of TiO_2, were sandwiched through O-rings between optical Pyrex plates. The solutions to be irradiated could circulate continuously from and to a gas tight reservoir. The distance between the optical plate and the membrane was 2 mm and the ratio between the overall reacting volume (in the photoreactor and in the reservoir) and the membrane surface area of the irradiated side was 1.1 mL cm^{-2}. The system was irradiated with UV light from a solar simulator (2.5 mW cm^{-2}). The initial photodegradation rate (Table **3**) resulted independent of the reactants and depended only on the photocatalyst amount and on the irradiance. The addition of H_2O_2 to the system increased markedly the photodegradation rate.

Table 3.   Initial Rate of Photodegradation of Chloroaliphatics Submitted to a Laboratory test with a Membrane-TiO_2-Photocatalytic Reactor [56]

Halo-organic Compound	Initial Rate of Photodegradation (μmol h^{-1})
Trichloroethene	5.9
Tetrachloroethene	5.7
Monochloroacetic acid	5.6
Dichloroacetic acid	5.9
Trichloroacetic acid	6.2

(*) mean of at least 6 kinetic runs (max deviation 0.6 μmol h^{-1}).

Other photodegradation experiments were carried out in a 10 kW pilot plant operating under an irradiance of 250 mW cm^{-2} in the UV range, employing a metallic membrane in the presence of 7 wt.% of photopromoter. The efficiency of the pilot plant was satisfactory by using methylene dichloride and trichlorethene as model pollutants.

4.1.4. Photocatalytic Membrane Reactor Combined with Wet Air Oxidation (WO2010021551A1)

The authors of patent [58] claim that photocatalysis in combination with some principles of the Watercatox process gives a unique configuration that facilitates the transport of molecules to the catalytic surface. The Watercatox process [59] combines catalytic wet air oxidation with a catalytic porous ceramic membrane gas-liquid contactor containing

catalyst nanoparticles; this makes possible oxidations in liquid phase at lower pressures (e.g. < 10 bar) and temperatures (< 80 °C) than those used in conventional wet oxidation and combustion processes [60]. In invention [58], the HP treatment can be achieved by illuminating a liquid/gas or liquid/liquid phase and a photocatalyst (under UV light) or a charge-transfer material (under visible light) separated from the other phase by the porous membrane acting as contactor. Fig. (**6**) shows a flow chart of a reactor according to this invention. The gas, liquid or suspension containing the pollutant contained in the tank (21) is pumped to the catalytic membrane contactor (22). The contactor is provided with glass windows (quartz or polymers with high transmittance) allowing irradiation of the membrane by the light source (23). The gas or liquid flows on one side of the catalytic membrane contactor. The second phase (oxidizing agent, reducing agent, etc.) is introduced to the other side of the catalytic membrane contactor. The outlet of the liquid or gas can be connected to a recycling line (24) to maintain the pressure or heat by flowing partial liquid or gas back to the feed tank (21). The catalytic membrane contactor can be constructed in flat, tubular, capillary, multichannel or other configurations.

Comparison of the claimed process with the Watercatox for oxidation of formic acid and humic acid oxidation indicated that the processes under light were much faster than the dark processes.

4.1.5. Modular Photocatalytic Reactor for Aquaculture Wastewater (EP1686095A1)

Another invention [61] presents a TiO_2-photocatalytic reactor with a modular configuration, using UV light and ozone, useful for purifying and disinfecting wastewater from confined aquaculture. The reactor, constructed in black polyethylene, has a cylindrical configuration; in the inner part, UV lamps and glass plates covered by supported TiO_2 are arranged. The reactor design features are:

1) A cylindrical configuration that facilitates its construction.

2) The supported catalyst is arranged in an annular type distribution around UV light lamps.

3) The modular configuration facilitates its assembly and maintenance and allows to handle different capacities and configurations (series and/or parallel) for wastewater treatment.

4) The reduced size facilitates the transport and installation of the device.

Fig. (**7**) shows a ground view of one of the support discs for the glass strips carrying the catalyst and opening holes of quartz tubes protecting the UV lamps. The main operational feature is that the reactor requires neither the recovery of the catalyst from the treated water nor thermophilic conditioning.

A laboratory assay was carried out for ammonium removal using a real water sample from a trout culture from the *Centro de Cultivo Piloto de la Universidad Católica de la Santísima Concepción (Concepción, Chile)*. The water culture was treated using photocatalysis and ozone. The process was very effective, achieving in two hours a removal
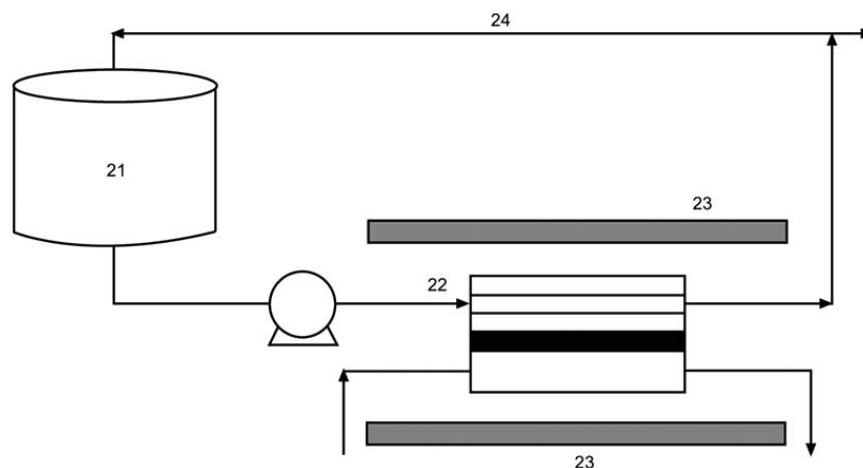
Fig. (6). Simplified scheme of the catalytic membrane reactor (adapted from [58]).
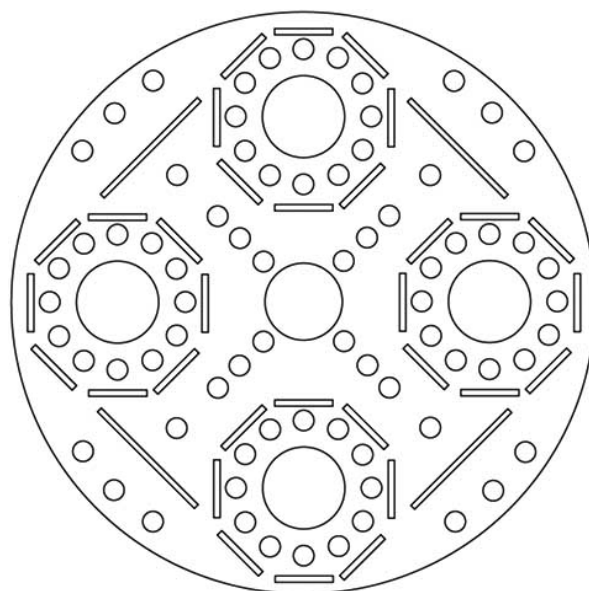

Fig. (7). Ground view of one of the support discs used in the invention for the glass strips carrying the catalyst and the opening holes of the quartz tubes, protecting the UV lamps [61].

of 58% of ammonium, total disinfection and a reduction of 50% of the dissolved organic matter. No other details of the experimental conditions are given.

4.1.6. Thin Film Fixed Bed TiO$_2$ Photocatalyst (WO2004058649A1)

Another invention [62] describes an apparatus for the photocatalytic oxidation of common industrial effluent contaminants in water using a solar driven thin film fixed bed reactor (TFFBR). The use of the process at large-scale is claimed. A thin film photocatalyst was fixed to an inert support using a simple spray technique. The support was Cuddapah stone, a construction material for houses obtained from Andhra Pradesh, a southern state in India. The photocatalytic films were easily prepared using a TiO$_2$ suspension (4 g in 100-200 mL water) and 1-5 mL of a binder (a surfactant, acrylic emulsion, resin or other polymers). The mixture was spread on the clean stone with a laboratory spray gun and left for drying; neither thermal treatment at high temperatures nor expensive precursors were needed. The coating

was repeated until a uniform aspect was obtained, not presenting pinholes. A common industrial effluent collected from a treatment plant at Hyderabad (Andhra Pradesh), containing nitrophenol, p-nitrotoluene sulfonic acid, paracetamol, p-aminophenol among other organic and inorganic compounds, was chosen to test the photoreactor. The effluent contained high COD (> 15000 mg L^{-1}), intense color and odor. After running the effluent through the TFFBR for 3 days under solar irradiation, a 50% of COD decrease was obtained, a similar value being obtained with a TiO$_2$ slurry (Fig. **8**).

4.2. PF Related Patents

As already said, in the photo-Fenton technology, immobilization of iron on convenient supports enhances the removal of organic pollution compared with the homogeneous technology, allowing at the same time to extend the working pH range.
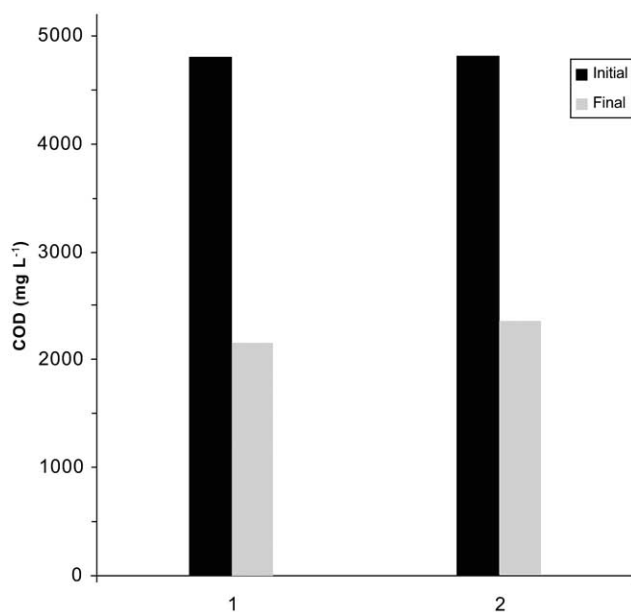
Fig. (8). COD reduction of an industrial common effluent. 1: TiO_2 in slurry, 2: with TFFBR over Cuddapah stone of the invention. Modified from [62].

4.2.1. Bentonite-iron nanocomposite for heterogeneous photo-Fenton (US20060076299A1)

A patent presents the synthesis of a bentonite (B) clay-based iron nanocomposite and its use as a heterogeneous PF catalyst to treat wastewaters from chemical and textile industries containing organic pollutants like azo-dyes [63]. The nanocomposite was made using the pillaring technique. For the synthesis, an Fe^{3+} pillaring solution was obtained by adding powdered $NaCO_3$ to an $Fe(NO_3)_3$ aqueous solution, added to an aqueous B suspension with vigorous stirring. Aging of the mixture was performed at room temperature or at 100 °C for 48 hours, followed by centrifugation and washing. In this way, a catalyst precursor forming intercalated bentonite iron oxide catalyst nanoparticles (Fe-B) was obtained.

The reactor was a cylindrical stainless steel vessel in whose inner wall surface Fe-B nanoparticles were sprayed to form a layer; a UV-C lamp (Philips 8 W, 254 nm) was inserted in the center of the vessel and H_2O_2 was added. Several tests to evaluate the performance of the Fe-B nanocomposites in PF treatments, using Orange II as model azo-dye pollutant, were performed. Fig. (**9**) shows the results obtained under different experimental conditions.

In the presence of Fe-B (curve b) in the dark, the very fast initial decrease of Orange II concentration was attributed to the adsorption of the azo-dye on the surface of the nanocomposite (adsorption capacity: ca. 20 mg Orange II per g of Fe-B). UV-C alone (a) yielded scarce removal. Under irradiation with only H_2O_2 addition (c), Orange II oxidation was significant due to the action of $HO^•$ coming from the H_2O_2 photolysis. In the Fenton dark system (d), discoloration was significant; however, the best results were obtained with the photo-Fenton treatment (e), allowing total discoloration in 1 h. Studies were performed to determine whether the faster
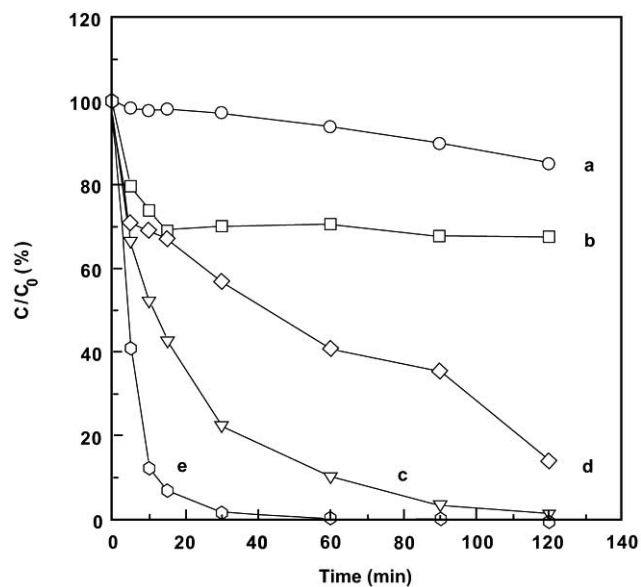

Fig. (9). Relative Orange II concentration *vs.* time. (a) Only UV-C irradiation; (b) in the dark, [Fe-B] = 1.0 g L^{-1}; (c) under irradiation without Fe-B and with addition of H_2O_2; (d) in the dark, [Fe-B] = 1.0 g L^{-1} with addition of H_2O_2; (e) under irradiation, [Fe-B] = 1.0 g L^{-1} with addition of H_2O_2. [Orange II] = 2.0 mM in all cases [63].

discoloration of Orange II was due to oxidation by $HO^•$ coming from the heterogeneous or from the homogenous photo-Fenton reaction, caused by the leaching of Fe from the Fe-B catalyst. Fe concentration in solution was measured under different experimental conditions and it was found that the amount of Fe passing to solution after 30 min of irradiation was very low in all cases, although the maximum (2.2 mg L^{-1}) corresponded to experiment (e). The authors concluded that the discoloration of Orange II is due to three processes: 1) adsorption on the Fe-B nanocomposite surface, 2) oxidation by heterogeneous PF reaction and 3) oxidation by homogenous PF reaction (having a minor role due to the low amount of Fe leached in solution).

4.2.2. Photo-Fenton Catalyst Supported Over HY-zeolite (US7407908B2)

Another patent [64] describes the preparation, characterization and evaluation of a claimed eco-friendly, efficient photo-Fenton catalyst with Fe(III) immobilized over an HY-zeolite support for use in the photocatalytic degradation of organic contaminants. Fe(III) ions were immobilized in different loadings (0.125-5 wt%) on HY zeolite by impregnation. A known weight of Fe(III) was dissolved in water and zeolite was added to this solution, soaked for 12 h under continuous stirring and dried at 100 ºC, followed by calcination at 450 ºC for 6 h in open air. The activity of the catalyst was evaluated by the degradation of phenol (Table **4**). The results clearly show that Fe(III)-HY is more efficient compared with the respective homogeneous PF process and this highlights the synergistic role of zeolite: the support not only brings the pollutant molecules closer to the vicinity of the photocatalyst but also stabilizes Fe(III)/Fe(II) ions through interaction in zeolite cavities. The use of heterogeneous Fe(III)-HY in the photo-Fenton reaction allows the use of a wider pH range

Table 4.   **Effect of Various Experimental Parameters on Photo-Fenton Degradation of Phenol (10^{-4} M); (A) UV + Fe(III)-HY + H_2O_2; (B) Homogeneous Photo-Fenton; (C) UV + Fe(III)-HY; (D) Dark + Fe(III)-HY + H_2O_2; (E) Photolysis [64].**

Time (min)	% Phenol				
	A	**B**	**C**	**D**	**E**
-30	100	100	100	100	100
0	86.9	99	85.7	86.2	100
30	6.2	63	75.7	83.5	97.7
60	1.5	48	74.6	80.9	93.6
90	-	35	72.3	79.8	92.8
120	-	27	69.6	78.1	91.3
150	-	24	64.7	78	89.8
180	-	20	-	-	-

Table 5. Effect of Fe(III) Loading over HY on Heterogeneous Photo-Fenton Degradation of Phenol (10^{-4} M); $H_2O_2 = 10^{-3}$ M; pH 6 [64].

Time (min)	% Phenol					
wt.% of Fe(III)-HY	**5**	**2**	**1**	**0.5**	**0.25**	**0.125**
-30	100	100	100	100	100	100
0	77.2	87.3	97.2	89	86.9	96.6
10	51.7	53.8	50.1	37	35.6	35.6
20	39.5	34.8	24.3	23	17.6	19.4
30	27.3	20.9	15.0	13	6.2	8.6
40	19.9	12	11.5	9	5.4	4.2
50	11.9	8	6.0	3.6	3.4	-
60	10.1	7.4	1.4	1.5	1.5	-

(up to 5-6) for the reaction against the narrow pH range needed in the homogeneous system. The catalyst, regenerated by calcination, could be reused at least for three cycles. Dissolution of Fe from the catalyst was low (0.1 to 4 mg L^{-1}). Table **5** describes the effect of Fe(III) loading over HY on phenol degradation. There is an optimum amount of Fe(III) (0.25 wt.%) that has to be incorporated to the zeolite to achieve an efficient degradation.

Results of phenol degradation over 0.25 wt% of Fe(III)-HY at pH 6 with different H_2O_2 concentrations indicate that with an increase of H_2O_2 from 10^{-4} to 10^{-3} M, removal increased due to increased $HO^{\bullet}$ in solution. Further increase to 10^{-2} M was detrimental, in agreement with the inhibitory role of H_2O_2 at high concentrations, as explained in section 2.1 of this paper.

4.2.3. *High Efficiency Heterogeneous Photo-Fenton Process (WO142724A1)*

Another invention presents the design of a heterogeneous photo-Fenton system for the abatement of organic pollutants in wastewater using heterogeneous perovskite-based cata-lysts, in both powder and in structured forms [65]. Three types of catalysts have been employed in the experimentation:

1) Bulk catalysts prepared by kneading powdered mixed oxides of elements of rare earths (e.g. La, Ce, Y, etc.) and a transition metal (Fe) with an alumina-based binder (aluminum hydroxide) in acid media, followed by extrusion of the plastic pastes to obtain a monolith catalyst, dried at 120 °C and calcined at 900 °C for 4 h. The catalytic activity of $LnFeO_3$ was studied by using acetic acid as model compound.

2) Supported catalysts prepared by impregnation of refractory monolithic honeycomb cordierite supports with solutions of precursors of perovskites, i.e. nitrate metallic salts ($LaMeO_3$, Me = Mn, Co, Fe, Ni, Cu or mixtures) in ethyleneglycol with added citric acid. The samples were taken out of the solution, dried in air and calcined at 900 °C for 4 h. Foams based on alumina or SiC were proposed to be used as supports.

3) A supported catalyst prepared by wet impregnation as reported in 2) with addition of Pt (as H_2PtCl_6). The substrate can be either pure or precovered by the oxide sublayer. After Pt loading, samples were dried under air or, before drying, treated with reducing species such as hydrazine hydrate.

The structured perovskite-based catalyst was tested with a variety of organic pollutants, including methyl-tert-butylether (MTBE), ethanol, methanol, their mixtures and synthetic winery wastewaters. The obtained results clearly indicated that the catalyst is more efficient than the homogeneous PF catalyst, due to the adsorption of the pollutant molecules on the surface of the catalyst. In addition, it allows enlarging the operative range of pH (e.g., pH 5) in comparison with the homogeneous system, without the formation of sludge. The photo-Fenton oxidation reaction was carried out in a single-pass reactor, in a batch reactor and in a continuous irradiated recirculated reactor, preferably sealed, as shown in Fig. (**10**).

The catalytic activity of the PF reaction was checked with one of the prepared catalysts, using a 2.5 g $LaFeO_3$ (2.24%) honeycomb monolith catalyst in 100 mL of acetic acid solution (0.021 M, TOC = 500 mg L^{-1}) and H_2O_2 (0.083 M (molar ratio: H_2O_2/acetic acid = 4), pH 3.9. An 8 W mercury vapor UV lamp was used. Samples were analyzed for TOC and H_2O_2. After 4 hours of irradiation, 55% TOC removal was observed, while the homogeneous system using ferric oxalate ($[Fe^{3+}]$ = 0.0296 M) yielded only 24% TOC removal. In the invention, pH, H_2O_2 conc. and H_2O_2 dosage have been optimized, and pH could be extended for acetic acid up to pH 6.

4.3. Patents Related to Combination of AOPs

4.3.1. Combined Treatment Technologies for Reclaimed Water (WO2009017756)

Pilot studies with a process including combinations of ozone, UV and H_2O_2 followed by pressurized microfiltration are presented in patent [66] for removal and destruction of contaminants present in regional US wastewaters. The interest was put, especially, in microorganisms and organic compounds, e.g. endocrine disruptive substances (N,N-diethyl-toluamide or DEET, ethynilestradiol, triclosan (TCS), etc.), pharmaceutically active compounds, pathogens (*Cryptosporidium*, poliovirus, coliforms) and other contaminants (nonylphenol (NP), bisphenol-A (BPA)). A UV/peracetic acid (PAA) system was an additional tested PAOP. The studies were designed to test the efficacy of different treatments for accurate prediction of the cost of full-scale implementation for setting up a 1-million gallon-per-day treatment facility.

In a pilot study (Dublin, CA), the impact of different ozone doses, the effect of H_2O_2 addition and of the quality of water using an ozone-based system was tested. Influent water was treated using a $HiPO_x$ reactor oxidation system in combination with either a microfiltration (MF) device or a sand filter. The $HiPO_x$ reactor was a 10 gallon-per-minute plug-flow-type reactor, which included H_2O_2 and O_3 injection points. The $HiPO_x$ process combines O_3 and H_2O_2 to form $HO^\bullet$ while controlling bromate formation, characteristic of high O_3 levels. The effluent was then filtered through a pressurized 0.2 μm pore size microfilter or a continuous backwash upflow sand filter (1.27-1.38 mm nominal sand media diameter, 80" media depth). The filtered effluent water was analyzed for particle size distribution, BOD (biological oxygen demand), pH/alkalinity, TSS (total suspended solids), turbidity, nitrate, ammonia and phosphate. MF was more efficient than sand to reduce the content of microorganisms in the size range of *Giardia, Crystosporidium* and bacteria and was also more effective in removing contaminants such as DEET, NP, TCS and BPA. Fig. (**11**) shows that virus removal is dependent on the applied ozone level but it is not affected by peroxide addition or type of filtration means. Similarly, coliform removal is affected by high ozone levels but not by H_2O_2 addition (Fig. **12**). It was established that effective coliform removal required higher levels of ozone than viruses.
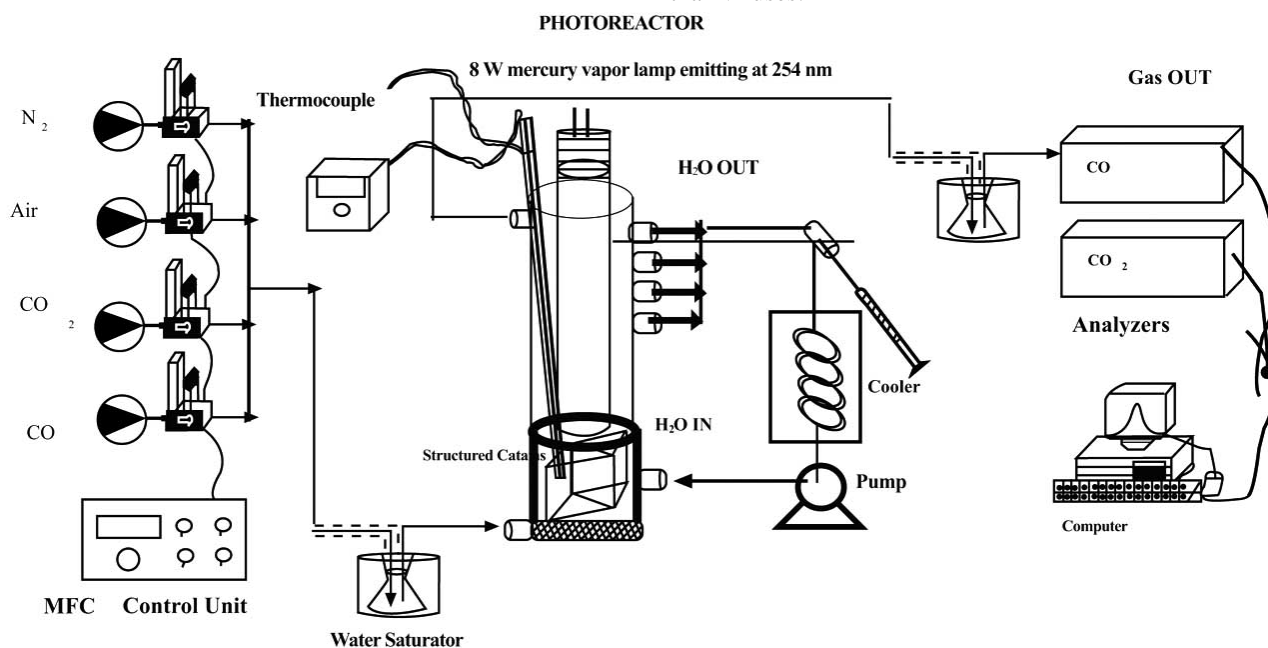

Fig. (10). Scheme of a laboratory recirculated reactor for the PF reaction of invention [65].
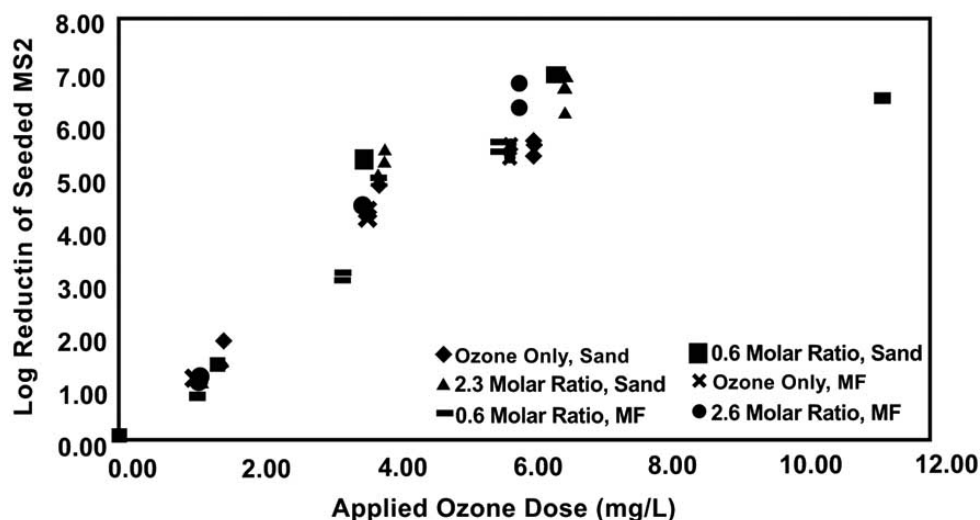
Fig. (11). Effect of ozone, peroxide and filtration on virus removal performed in pilot studies Dublin, CA, USA, according to invention [66].
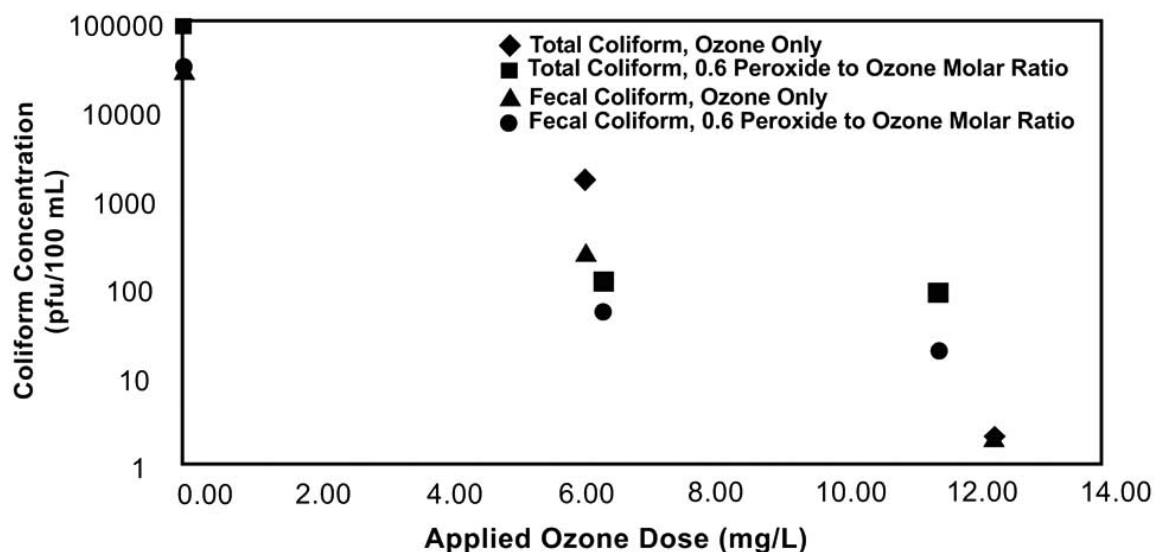

Fig. (12). Effect of ozone and peroxide levels on the efficiency of coliform removal performed in pilot studies Dublin, CA, USA, according to invention [66].

High levels of O_3 promote bromate formation, but removal of bromate can be accomplished by H_2O_2. Fig. (**13**) shows the effect of ozone levels on removal of NP, TCS and BPA. It can be seen that ozone provides substantial destruction of NP, triclosan and BPA. The results show that HiPOx treatment can be coupled with MF to remove effectively organic compounds and pathogens.

In a second plant (Pinellas county, FL, USA), the impact of UV dose and H_2O_2 addition on contaminant removal was determined. The reactor was a UV/peroxide pilot Trojan (London, Ontario, Canada) equipment, with 30 low-pressure, high-output UV lamps and a H_2O_2 injection system. The particular pollutants of this study were estradiol compounds and the potent carcinogen N-nitrosodimethylamine (NDMA). Results indicate that increasing levels of O_3 increased destruction of EEQ (estrogen equivalent), while the type of filtration had little effect. Increasing levels of H_2O_2 increased destruction of EEQ while the amount of UV exposure had minimal effect. Both UV and H_2O_2 treatment reduce NDMA levels. Increasing H_2O_2 concentration above 5

mg L^{-1} minimally increased NDMA destruction, suggesting that the optimal efficiency can be achieved at moderate H_2O_2 levels. H_2O_2 did not affect UV virus disinfection: increasing amounts of H_2O_2 failed to reduce the levels of MS2 phage more than UV alone. As a conclusion, in this invention, UV treatment for virus destruction can be combined with ozone and/or H_2O_2 for EEQ and NDMA destruction.

A third plant in Bradenton (FL, USA) was employed to determine the impact of PAA/UV and UV/H_2O_2 on removal. The study demonstrated again that MF, after PAA/UV or UV/H_2O_2, provided a substantially better microorganism barrier than sand filtration. Addition of O_3 at high doses satisfied the coliform criteria of California Code (2.2 MPN per 100 mL total coliforms). Ozone at even moderate doses provided substantial virus destruction. On the other hand, O_3 and O_3/H_2O_2 provided substantial contaminant destruction, and H_2O_2 further reduced disinfection byproducts (DBP). The results of this third plant suggested that combinations of UV/O_3/H_2O_2 can be used to remove a diverse range of contaminants, taking advantage of the decontamination proper-
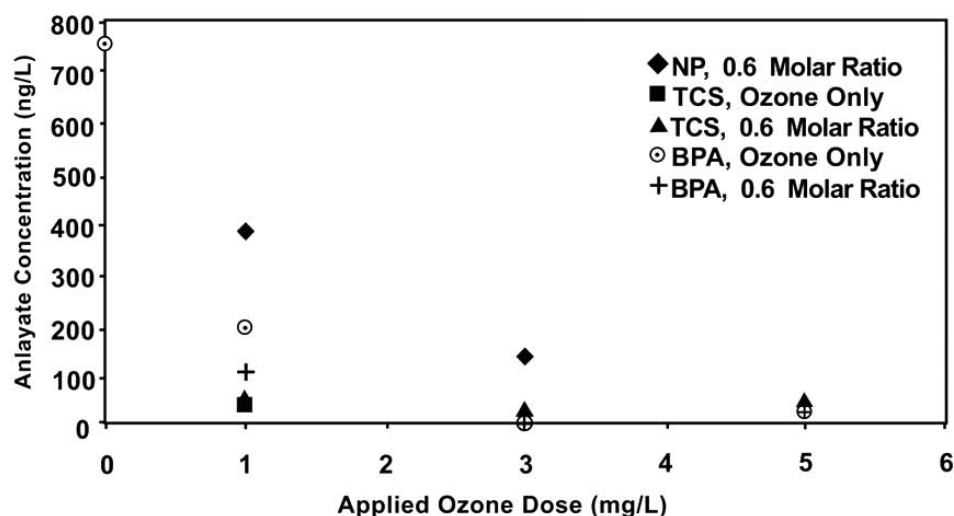
Fig. (13). Effect of ozone levels on removal of NP, TCS and BPA performed in pilot studies Dublin, CA, USA according to invention [66].

ties of each treatment and exploiting the formation of HO$^\bullet$ produced by UV/H$_2$O$_2$ and O$_3$/H$_2$O$_2$ combinations.

Based on the pilot studies, a cost estimate for setting up a 1-million gallon-per-day treatment facility was prepared. While the treatment with sand and chlorine is the least expensive, the limited ability of sand to filter microcontaminants and the undesirable taste and odor associated with chlorine limit the efficacy of the method. While conventional ultrafiltration (UF), RO and AOPs are more effective, the cost of these methods can be prohibitive. The studies suggest that ozone and UV combined with H$_2$O$_2$ and MF can adequately decontaminate wastewater at a fraction of the cost of conventional methods, and even substitute conventional methods (Fig. **14**).

4.3.2. Treatment of Water for Zero Liquid Discharge Plants (US7531096B2)

Zero Liquid Discharge (ZLD) systems are used in power industry to address problems associated with limitations of water availability, conservation of fresh water supplies and environmental restrictions on discharge. The aim of patent [67] is to produce clean feed water for a boiler system of a power plant configured for ZLD by reducing the organic contaminants in the source water (TOC < 300 µg L^{-1}), employing a pressurized advanced oxidation system in continuous operational mode. The system (Fig. **15**) includes an ozonation module (25) for applying ozone at high concentration to the source water followed by an ozone reactor (26) in which the mixed stream is retained under pressure, connected to a UV reactor (27) downstream for enhanced contaminant reduction, and a retention tank (28).

As explained before, the rate of organic contaminant conversion depends on the mass transfer of O$_3$ from the gas to the liquid phase. In this way, important controls on ozone transfer efficiency include pressure, temperature, reaction time, ionic strength and ozone feed. It is also necessary to use ozone destructor systems to eliminate the excess of ozone not dissolved in the liquid stream, which cannot be discharged into the atmosphere. The system includes two on-line TOC analyzers (one before and another after the treatment) configured to determine TOC levels in a near real-

time. The second TOC analyzer can be used to compare the obtained TOC level with the maximum limit established and, if it is exceeded, the effluent can be directed back to the ozonation module.

4.3.3. Multi-barrier Water Purification System (WO2009044288A2)

In another patent [68], a method integrating UV radiation in an advanced decontamination processes and a honing material, along with a cross-flow membrane filter (usually a ceramics) into a single closed-loop system, is described. One of the important achievements of the offered technique is that it provides a 100% fluid recovery system, *i.e.* zero reject stream. In one of the embodiments, a filtration membrane and a honing material are located in the effluent to scrub foulants from the membrane. The system comprises an advanced decontamination process sufficient to destroy, by oxidation or reduction, biological and organic contamination. The authors claim that such a combination has not been provided in conventional approaches, and that the system presents enhanced performance over the sum of the individual technologies. In a more specific closed-loop system, a cross-flow filtration membrane and a TiO$_2$ photocatalytic slurry are placed in the contaminated aqueous system. In this case, the slurry has a texture sufficient to scrub foulants from the filtration membrane and acts as honing material. The system includes a UV light source providing a photolytic reaction sufficient for disinfection and it can be located in any place in the closed-loop system. Addition of H$_2$O$_2$ and O$_3$ can increase the decontaminating power of the system. In other cases, the honing may be provided by a honing material and/or by turbulent flow within the reactor. The membrane acts as an ultimate barrier for most biological species. A "blowdown" can be incorporated to eliminate suspended solids within the loop. A fourth barrier such as RO or electrodialysis may also be added to the output of the multi-barrier system to remove inorganic salts, etc. The system not only disinfects but also sterilizes: algae, protozoa, mold spore, bacteria or viruses cannot pass the ceramic cross-flow filter membrane. The implementation of the multi-barrier system might eliminate the use of more complicating tech-
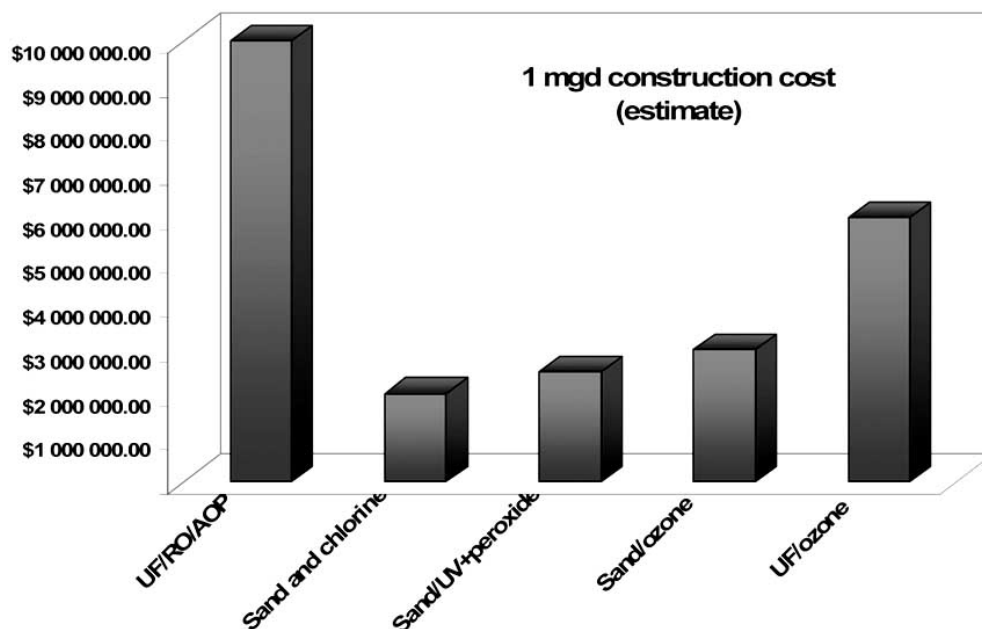
Fig. (14). Comparison of the construction costs of different water treatment facilities studied in invention (adapted from [66]).
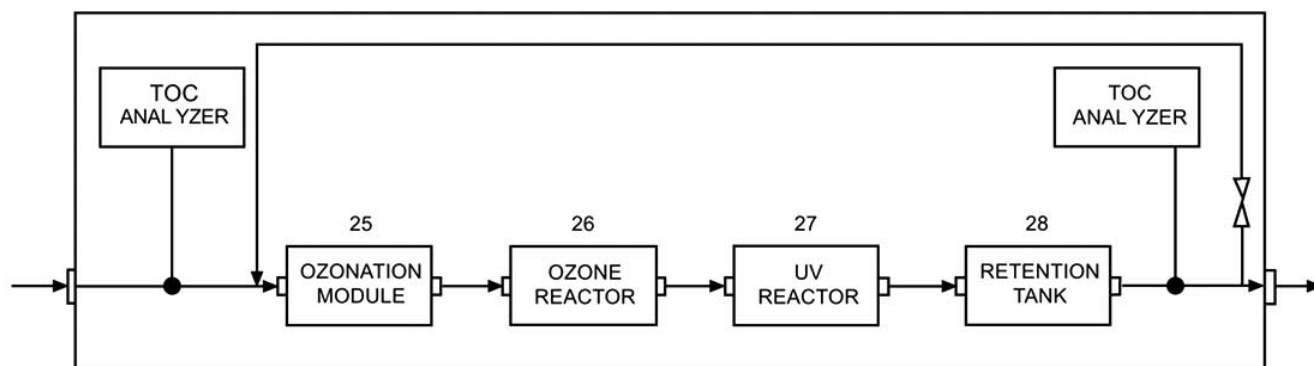

Fig. (15). Scheme of the advanced oxidation system employed to produce clean feed water production for a boiler system of a power plant configured for ZLD, according to patent (adapted from [67]).

nologies such as flocculation-coagulation-clarification, chemical precipitation, MF & UF, sand filtration, activated carbon adsorption, UV disinfection, greensand filters, etc. It is claimed that the filtration membrane, having dynamic filter coating, can treat 2000 gal ft^{-2} per day with an effective filtration pore size about 12 nm. Summarizing, the multi-barrier system destroys and mineralizes organic compounds, removes suspended solids, reduces turbidity, color, odor and even remove some heavy metals, and it is proposed to treat drinking water or water for reuse. All the steps are performed in a stand-alone unit with inlet and outlet for the fluid. A scheme of the proposed system is shown in Fig. (**16**).

4.3.4. Process for Treatment of Large Amounts of Vinasse Wastewater (WO2009135276A1)

In patent [69], a process for treatment of large amounts of wastewater of vinasse, a toxic liquid residue abundantly produced on ethanol manufacturing or alcoholic beverage production, is proposed. In the case of sugar cane, vinasse is generated on large amounts, from 10 to 18 L per liter of produced alcohol. The wastewater leaves the distillation appara-

tus at 85-90 ℃, with an elevated amount of pollutants (mainly recalcitrant phenolic compounds), considerable organic charge (high COD and BOD), intense coloring and low pH, being highly toxic to the flora and fauna. In addition, the slow natural degradation exhales strong and unpleasant toxic odors. The proposed disinfection and degradation process consisted on the sequential application of different stages: oxidation, biodigestion, neutralization, coagulation, flocculation, photooxidation by AOPs and demineralization by absorption. The authors claim that the resulting wastes can be utilized as fertilizers and nutrients, the biogas as energy source, and the recycled water for irrigation or other purposes.

The first stage is an ozonation process for oxidation of organic recalcitrant pollutants. When ozone is sparkled for several minutes, 50-80% oxidation of the phenolic components is achieved, enough to allow the effluent entering the biological treatment. The second stage consists in the passage through a bioreactor such as UASB (Upflow Anaerobic Sludge Blanket)-type, mixed bed anaerobic filters, fixed bed
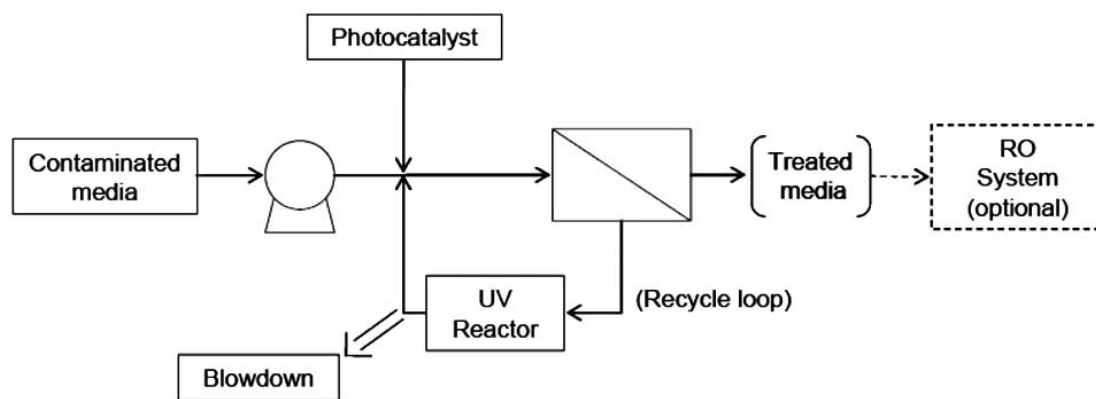
Fig. (16). Scheme of a closed-loop multi-barrier cross flow-filtration system integrated with AOP proposed in innovation (modified from [68]).

anaerobic filters, ascending or descending, with polymeric, clayish, zeolitic beds or even vegetal fibers or sponges (*Luffa cilindrica*) at a very slow flow. Mesophyll anaerobic microorganisms show a great performance for this purpose. The obtained biogas is recycled and used on heating parts of the plant or as a fuel. In the third stage, the effluent is submitted to a coagulation-flocculation process where a substantial part of the colloidal organic charge is separated from the fluid phase with simultaneous elimination of turbidity. Hydroxides, oxides or carbonates from alkaline or alkaline earth metals or ferrous sulfate can be used in this stage. The supernatant fluid is then submitted to the fourth stage, a PAOP like photo-Fenton, UV/ozone, UV/H_2O_2, or TiO_2- or ZnO-photocatalysis. The remaining fluid already contains low levels of BOD. In the last stage, removal of inorganic ions is performed through adsorbents/ionic exchangers like resins, zeolites, clays, bentonites, kaolin derivatives, molecular sieves, etc. In this way, the organic charge is reduced 95-100% and COD 90-100%, with an important increase on BOD_5/COD (biodegradability index).

4.3.5. Embedded Electron Induced Ozonation and Activation of Nanostructured TiO_2 (US7691342B2)

A recent invention [70] proposes a process using compact embedded electron induced ozonation and activation of nanostructured TiO_2 useful for photocatalytic oxidation of alcohols, hydrocarbons or other organic pollutants. The authors claim that by selectively producing partial oxygenates and less by-products and pollutants than conventional oxidation reactions, the process achieves economy of the atomic level by direct oxygenation of hydrocarbons without using multiple stages and without loss of atoms.

The system is a unitary apparatus, based on the use of an emitting UV light surface corona, which produces ozone and activates a photocatalyst coated on the surface. Surface corona is an electrical discharge (frequently luminous, non-thermal plasma) at the surface of a conductor or between two conductors of the same transmission line, accompanied by ionization of the surrounding atmosphere. The surface corona discharge system produces O_3 by passing air or O_2 through a high voltage electrical discharge (> 5000 V). Surface corona generates low energy electrons (10-20 eV), which are accelerated, collide with O_2 and dissociate the

molecular bond in two free oxygen atoms; their collision with other oxygen molecules creates ozone. A surface corona discharge also produces UV light of low power (about 2.0 W). Several references on the fundamentals and applications of surface corona are included in the patent (see for example [71-76]). Ozone concentrations of 1-2% using air, and 3-8% using oxygen can be obtained by surface corona discharge generators. The photocatalyst is a thin film of nanoparticulate TiO_2 (primary particle size: 0.02-0.2 μm), deposited on a substrate by a flame aerosol method. In one example of the application, the method was employed for the treatment of water contaminated with MTBE. Fig. (**17**) is a cross-sectional schematic diagram of the prototype surface corona discharge photocatalytic reactor used in this working example.

The reactor consisted of two concentric tubes (29) and (30). The outer tube (29) had embedded ceramic electrodes on its inner surface, which generate UV light. The inner Pyrex tube (30) had its inner surface coated with a nanostructured film, prepared by deposition of a fine-grained, high-surface area TiO_2 (98% anatase, 33 nm crystallite size, 80-100 m^2 g^{-1}). The generated UV light passed through tube (30) and activated the TiO_2 film in contact with the MTBE contaminated water. Ozone was supplied through fritted glass at the bottom of tube (30) and percolated up through the contaminated water within the reactor. SEM (scanning electron microscopy) images of the TiO_2 film indicate that the material had an uneven granular surface, providing many adsorption sites for MTBE. The TiO_2 film was found to adhere very well to the Pyrex tube and was very durable throughout several runs. The ozone concentration and UV light intensity were adjusted with a variable voltage control. Varying these parameters allowed determination of the role of each AOP on MTBE degradation, along with the synergistic effect of using both processes together. The irradiance of the generated UV light, measured with a radiometer/photometer was 2.5 and 12 mW cm^{-2} for 315-400 nm and 250-315 nm, respectively. Fig. (**18**) presents the results of the experiments conducted under different conditions. The enhanced effect of TiO_2 photocatalysis was more noticeable with a low ozone concentration, and with a high ozone concentration, there was no significant enhancement of MTBE degradation by the combined effects. The advantage of the
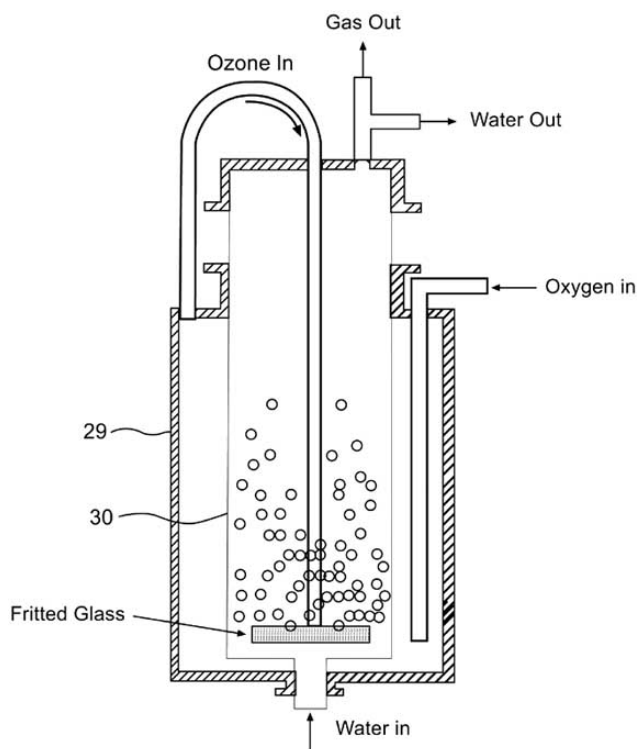
Fig. (17). Schematic view of the combined liquid phase reactor for ozonation and photocalytic oxidation of MTBE [70].
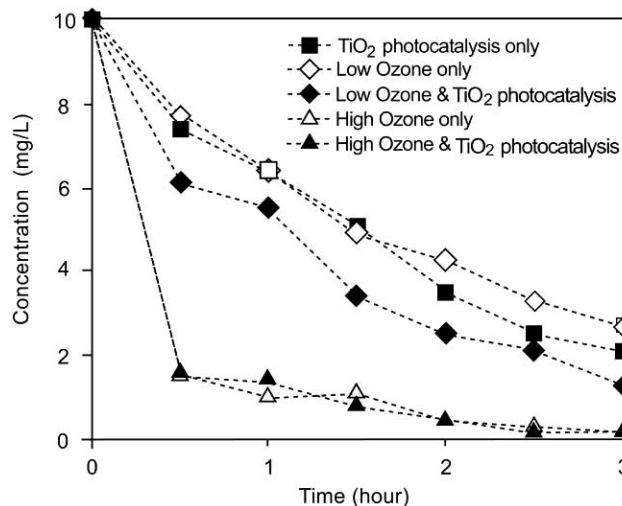

Fig. (18). Concentration of MTBE *vs.* time under different conditions in experiments performed with the system of patent [70].

invention is that the surface corona originates simultaneously ozone and UV light, causing a synergistic effect for oxidation. Additionally, the surface corona discharge generator accelerates electrons and produces free radicals and ions, able to provoke additional oxidation reactions.

4.3.6. Regeneration of Adsorbents by AOPs (WO2007056717A2)

A recent patent proposes the use of zeolites as hosts to entrap organics inside the adsorbent pores of hydrophobic molecular sieves, submitting then the materials to AOPs to regenerate the adsorbents, by removing of bound contaminants [77]. Coupling these two processes, the method leads to ultimate destruction of the contaminants. Particular examples of zeolites used in the invention are siliealite-1, dealuminated zeolite Y (DAY) and mordenite. Using hydrophobic molecular sieves, the disadvantages of common activated carbon or other adsorbents (low capacity, competition of NOM, high temperature regeneration costs or costly disposal) are avoided due to the smaller pore size that makes them more selective for organic removal. Some of the advantages of this invention include:

1) Much smaller processing volumes.

2) Water is never in contact with the advanced oxidation reagents.

3) Organics are mineralized to safer end-products (CO_2 + H_2O).

4) Reduced oxidant doses.

5) Hydrophobic molecular sieves can be reused repeatedly after regeneration.

The proposed oxidation reagent may be O_3 or combined technologies such as O_3/H_2O_2, Fe^{2+}/H_2O_2, zerovalent iron/H_2O_2, etc. The method can be designed as sequential removal/regeneration systems, continuous flow systems or simultaneous removal/treatment systems using a single-step process. The system was proposed to treat organic compounds like MTBE, trichloroethylene, BTEX (benzene, toluene, ethylbenzene, and xylenes), etc. The adsorbents are affixed to a substrate, like a permeable membrane (a polycrystalline particulate aggregate) and they are removed from the water by centrifugation or filtration.

In one example, silicalite-1 and DAY removed successfully DBPs like chloroform (CLF) and trichloroacetic acid at low concentrations after 24 h contact time on an orbital shaker (0.2 g sorbent in 40 mL solution). However, the contaminants remained in the sorbents in concentrated form after adsorption. For regeneration, the zeolite was directly coated with zerovalent iron by a borohydride reduction procedure starting from $FeSO_4.7H_2O$. The Fe^0 coated adsorbent was then subjected to 30% H_2O_2. The adsorbent was subjected to repeated cycles of adsorption followed by regeneration. Fig. (**19**) indicates that repeated adsorption of CLF to silicalite-1 resulted in saturation of the solid, with no further CLF uptake after 7 cycles (0.2 g adsorbent in 40 mL solution containing initially 1 mg L^{-1} CLF). However, submitting the material to advanced oxidation just adding H_2O_2 after each cycle, resulted in constant capacity for adsorption.

The authors claim that the process can be also performed under UV irradiation, by a photo-Fenton process or other PAOPs.

5. CURRENT & FUTURE DEVELOPMENTS

AOPs appear as very strong and important technologies to be employed in water and wastewater treatment in very especial cases, when very recalcitrant compounds are present, which cannot be destroyed or transformed by conventional technologies into less noxious chemical compounds. From AOPs, those based on photochemical processes
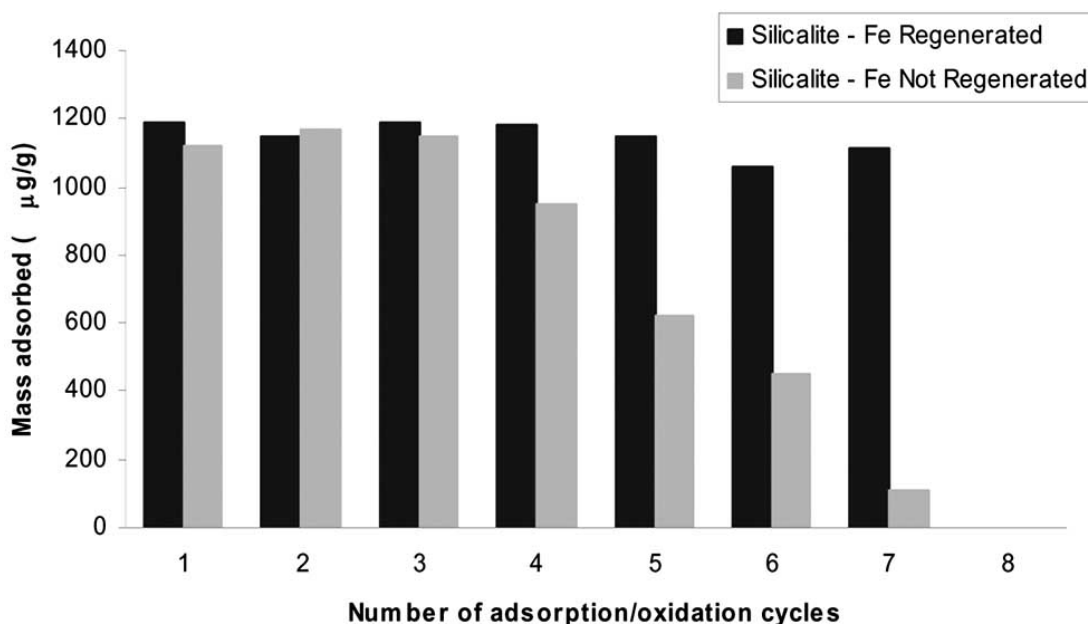
Fig. (19). Regeneration of Fe^0-coated silicalite-1 with H_2O_2 after CLF contact ([77]).

(PAOPs) are the most studied because the required energy is not as expensive as in the case of more sophisticated methods, e.g. those using high temperature and pressures or radiolytic processes. The final aim, always wished, is the mineralization of organic compounds to CO_2 plus H_2O and other simple inorganic substances. However, this final aim is seldom achieved and only some AOPs, in very especial conditions, can attain this ultimate goal. It is important to remark also that only small or medium volumes can be treated by these technologies.

Many academic studies on PAOPs have been made, generally using one single model pollutant, which achieved the complete elucidation of mechanisms and identification of intermediate compounds formed in the systems, together with the kinetic regimes taking place. Also, engineering models and design of reactors are rather well developed and can be found in the literature. In spite of all these findings, AOPs have not been very much applied in real systems, and not many patents on the subject appear in the literature. Among them, photocatalytic oxidation and photo-Fenton treatment, combined or alone, appears to be one step ahead in terms of technological development. It can be observed that most of the patented work relies on one of the biggest problems when using photocatalytic techniques for water purification or treatment, which is the necessity of fixing the photocatalyst to a convenient support to avoid a further costly separation. In other cases, combination of technologies appears as the most feasible application, using the synergy of simultaneous technologies or the increase of the degradation at the least cost by application of successive technological steps.

Two final conclusions follow. First, only a few authors focus on the actual operating cost of the technologies and more detailed cost analysis should be performed, since the information is fundamental to choose a water treatment system. Second, although most applied and patented works claim that their proposed methods can be used in a general

way, or that the combinations may be extended and even "universal", it is always mandatory to perform a treatability study of the waters before real application of the technologies.

As sophisticated and complex devices are hard to be developed and used by water and wastewater managers, future developments should focus on simple, non-expensive, easily constructed and easily handled systems. Systems to provide safe and clean water to isolated populations should be also considered by technologists.

CONFLICT OF INTEREST

None.

ABBREVIATIONS

A	=	Acceptor
AO7	=	Acid Orange
AOP	=	Advanced Oxidation Process
AOT	=	Advanced Oxidation Technology
B	=	Bentonite
BOD	=	Biological oxygen demand
BPA	=	Bisphenol-A
BTEX	=	Benzene, toluene, ethylbenzene, and xylenes
CFD	=	Computational fluid dynamics
CLF	=	Chloroform

COD	=	Chemical oxygen demand
D	=	Donor
DAY	=	Dealuminated zeolite Y
DBP	=	Disinfection byproducts
DEET	=	N,N-diethyl-toluamide
DOC	=	Dissolved organic carbon
e_{cb}^{-}	=	Conduction band electrons
EDTA	=	Ethylenediaminetetraacetic acid
E_{EO}	=	Electrical energy per order
EEQ	=	Estrogen equivalent
E_g	=	Bandgap
Fe-B	=	Bentonite iron oxide catalyst nanoparticles
FHO	=	Fresh iron oxyhydroxides
Gal	=	Gallic acid
$HO^{\bullet}$	=	Hydroxyl radical
$HO_2^{\bullet}$	=	Hydroperoxyl radical
HP	=	Heterogeneous photocatalysis
h_{vb}^{+}	=	Valence band holes
L	=	Ligand
LED	=	Light-emitting diode
LMCT	=	Ligand to metal charge transfer
MF	=	Microfiltration
MTBE	=	Methyl-tert-butylether
NDMA	=	N-nitrosodimethylamine
NOM	=	Natural organic matter
NP	=	Nonylphenol
NZVI	=	Zerovalent iron nanoparticles
PAA	=	Peracetic acid
PAOP	=	Photochemical Advanced Oxidation Process
PET	=	Polyethyleneterephtalate
PF	=	Photo-Fenton
pH_{pzc}	=	Point of zero charge
PMR	=	Photocatalytic membrane reactor
RO	=	Reverse osmosis
ROS	=	Reactive oxygen species
SEM	=	Scanning electron microscopy
SORAS	=	Solar Oxidation and Removal of Arsenic
TCS	=	Triclosan
TFFBR	=	Thin film fixed bed reactor
TOC	=	Total organic carbon
TSS	=	Total suspended solids
UASB	=	UPFLOW Anaerobic Sludge Blanket

UF	=	Ultrafiltration
US	=	Ultrasound
UV	=	Ultraviolet
V_{fb}	=	Flatband potential
VUV	=	Vacuum ultraviolet
ZLD	=	Zero Liquid Discharge
ZVI	=	Zerovalent iron
ϕ	=	Quantum yield
ε	=	Molar absorption coefficient M^{-1} cm^{-1}

REFERENCES

[1] Buxton GV, Greenstock CL, Helman WP, Ross AB, Tsang W. Critical review of rate constants for reactions of hydrated electrons, Chemical kinetic data base for combustion chemistry. Part 3: Propane. J Phys Chem Ref Data 1988; 17: 513-886.

[2] Glaze WH, Kang JW, Chapin DH. The chemistry of water treatment processes involving ozone, hydrogen peroxide, and ultraviolet radiation. Ozone Sci Eng 1987; 9: 335-42.

[3] Oppenländer T. Photochemical purification of water and air. Weinheim, Germany: Wiley-VCH 2002.

[4] US/EPA Handbook of advanced photochemical oxidation processes. EPA/625/R-98/004, 1998.

[5] Legrini O, Oliveros E, Braun AM. Photochemical processes for water treatment. Chem Rev 1993; 93: 671-98.

[6] Pignatello JJ, Oliveros E, MacKay A. Advanced oxidation processes for organic contaminant destruction based on the Fenton reaction and related chemistry. Crit Rev Environ Sci Technol 2006; 36: 1-84.

[7] Hoffmann MR, Martin ST, Choi W, Bahnemann DW. Environmental applications of semiconductor photocatalysis. Chem Rev 1995; 95: 69-96.

[8] Fujishima A, Rao TN, Tryk DA. Titanium dioxide photocatalysis. J Photochem Photobiol C 2000; 1: 1-21.

[9] Litter MI. Heterogeneous photocatalysis. Transition metal ions in photocatalytic systems. Appl Catal B 1999; 23: 89-114.

[10] Doménech D, Jardim W, Litter M. Tecnologías avanzadas de oxidación para la eliminación de contaminantes. In: Blesa MA, Sánchez B, Eds. Eliminación de Contaminantes por Fotocatálisis Heterogénea: Ediciones CIEMAT 2004; pp. 7-34.

[11] Litter MI. Introduction to photochemical advanced oxidation processes for water treatment. In: Bahnemann D, Boule P, Eds. The Handbook of environmental chemistry, series, Volume M, Part L: Environmental Photochemistry Part II. Springer-Verlag: GmbH Publish 2005; pp. 325-66.

[12] Litter MI. Treatment of chromium, mercury, lead, uranium and arsenic in water by heterogeneous photocatalysis. In: De Lasa H, Serrano B, Eds. Advances in chemical engineering, photocatalytic technologies. Elsevier: Academic Press 2009; vol. 36: pp. 37-67.

[13] Gogate PR, Pandit AB. A review of imperative technologies for wastewater treatment I: oxidation technologies at ambient conditions. Adv Environ Res 2004; 8: 501-51.

[14] Gogate PR, Pandit AB. A review of imperative technologies for wastewater treatment II: hybrid methods. Adv Environ Res 2004; 8: 553-97.

[15] Braslavsky, SE. Glossary of terms used in photochemistry. 3rd ed. Pure Appl Chem 2007; 79: 293-465.

[16] Alpert SM, Knappe RUD, Ducoste JJ. Modeling the UV/hydrogen peroxide advanced oxidation process using computational fluid dynamic. Water Res 2010; 44: 1797-808.

[17] Cisneros LR, Espinoza GA, Litter MI. Photodegradation of an azo dye from the textile industry. Chemosphere 2002; 248: 393-9.

[18] Mohey el-Dein A, Libra JA, Wiesmann U. Mechanism and kinetic model for the decolorization of the azo dye Reactive Black 5 by hydrogen peroxide and UV radiation. Chemosphere 2003; 53: 1069-77.

[19] Behnajady MA, Modirshahla N, Shokri M, Vahid B. Design equation with mathematical continuous-flow photoreactor. J Hazard Mater 2009; 165: 168-73.

[20] Bolton JR, Bircher KG, Tumas W, Tolman CA. Figures-of-merit for the technical development and application of advanced oxidation technologies for both electric- and solar-driven systems (IUPAC technical report). Pure Appl Chem 2001; 73: 627-37.

[21] Aleboyeh A, Olya ME, Aleboyeh H. Electrical energy determination for an azo dye decolorization and mineralization by UV/H₂O₂ advanced oxidation process. Chem Eng J 2008; 137: 518-24.

[22] Augugliaro V, Litter M, Palmisano L, Soria J. The combination of heterogeneous photocatalysis with chemical and physical operations: a tool for improving the photoprocess performance. J Photochem Photobiol C 2006; 7: 127-44.

[23] Domènech X, Casado J, Peral J. Solar activated ozonation of phenol and malic acid. Chemosphere 2003; 50:1085-93.

[24] Chen R, Pignatello JJ. Role of quinone intermediates as electron shuttles in Fenton and photoassisted Fenton oxidations of aromatic compounds. Environ Sci Technol 1997; 731: 2399-466.

[25] Kim SM, Geissen SU, Vogelpohl A. Landfill leachate treatment by a photoassisted Fenton reaction. Water Sci Technol 1997; 35: 239-48.

[26] Hermosilla D, Cortijo M, Huang CP. The role of iron on the degradation and mineralization of organic compounds using conventional Fenton and photo-Fenton processes. Chem Eng J 2009; 155: 637-46.

[27] Linsebigler AL, Lu G, Yates JT Jr. Photocatalysis on TiO₂ surfaces: principles, mechanisms and selected results. Chem Rev 1995; 95: 735-58.

[28] Mills A, Le Hunte SJ. An overview of semiconductor photocatalysis. J Photochem Photobiol A 1997; 108: 1-35.

[29] Fujishima A, Zhang X. Titanium dioxide photocatalysis: present situation and future approaches. C R Chimie 2006; 9: 750-60.

[30] Martin ST, Herrmann H, Hoffmann MR. Time-resolved microwave conductivity Part 2.-Quantum-sized TiO₂, and the effect of adsorbates and light intensity on charge-carrier dynamics. J Chem Soc Faraday Trans 1994; 90: 3323-330.

[31] Ibáñez JA, Litter MI, Pizarro RA. Photocatalytic bactericidal effect of TiO₂ on *Enterobacter cloacae*. Comparative study with other Gram (-) bacteria. J Photochem Photobiol A 2003; 157: 81-5.

[32] Emilio CA, Testa JJ, Hufschmidt D, *et al*. Features and efficiency of some platinized TiO₂ photocatalysts. J Ind Eng Chem 2004: 10; 129-38.

[33] Fujishima A, Zhang X, Tryk DA. TiO₂ photocatalysis and related surface phenomena. Surf Sci Rep 2008; 63: 515-82.

[34] Meichtry JM, Rivera V, Di Iorio Y, Román SE, Grela MA, Litter MI. Photoreduction of Cr(VI) using hydroxoaluminumtricarboxymonoamide phthalocyanine adsorbed on TiO₂. Photochem Photobiol Sci 2009; 8: 604-12.

[35] Litter MI, Morgada ME, Bundschuh J. Possible treatments for arsenic removal in Latin American waters for human consumption. Environ Pollut 2010; 158: 1105-18.

[36] Morgada ME, Levy IK, Salomone V, Farías SS, López G, Litter MI. Arsenic (V) removal with nanoparticulate zerovalent iron: effect of UV light and humic acids. Catal Today 2009; 143: 261-8.

[37] Bundschuh J, Litter M, Ciminelli V, *et al*. Emerging mitigation needs and sustainable options for solving the arsenic problems of rural and isolated urban areas in Iberoamerica - A critical analysis. Water Res 2010; 44: 5828-45.

[38] Noubactep C. Processes of contaminant removal in "Fe⁰-H₂O" systems revisited: the importance of co-precipitation. Open Environ J 2007; 1: 9-13.

[39] Hug S, Canonica L, Wegelin M, Gechter D, von Gunten U. Solar oxidation and removal of arsenic at circumneutral pH in iron containing waters. Environ Sci Technol 2001; 35: 2114-21.

[40] Emmett MT, Khoe GH. Photochemical oxidation of arsenic by oxygen and iron in acidic solutions. Water Res 2001; 35: 649-56.

[41] Pulgarin C, Sarria V, Kenfack S, Guillod O. An innovative coupled solar-biological system at field pilot. J Photochem Photobiol A 2003; 159: 89-99.

[42] Oller I, Malato S, Sanchez-Perez J, *et al*. A combined solar photocatalytic-biological field system for the mineralization of an industrial pollutant at pilot scale. Catal Today 2007; 122: 150-9.

[43] Kitis M, Adams CD, Daigger GT. The effects of Fenton's reagent pretreatment on the biodegradability of nonionic surfactants. Water Res 1999; 33: 2561-8.

[44] de la Fuente L, Acosta T, Babay P, Curutchet G, Candal R, Litter MI. Degradation of nonylphenol ethoxylate-9 (NPE-9) by photo-

chemical advanced oxidation technologies. Ind Eng Chem Res 2010; 49: 6909-15.

[45] Lucas MS, Peres JA, Li Puma G. Treatment of winery wastewater by ozone-based advanced oxidation processes (O₃, O₃/UV and O₃/UV/H₂O₂) in a pilot-scale bubble column reactor and process economics. Separ Purif Technol 2010; 72: 235-41.

[46] Quici N, Morgada ME, Piperata G, Babay P, Gettar RT, Litter MI. Oxalic acid destruction at high concentrations by combined heterogeneous photocatalysis and photo-Fenton processes. Catal Today 2005; 101: 253-60.

[47] Quici N, Morgada ME, Gettar R, Bolte M, Litter MI. Photocatalytic degradation of citric acid under different conditions: TiO₂ heterogeneous photocatalysis against homogeneous photolytic processes promoted by Fe(III) and H₂O₂. Appl Catal B 2006; 71: 117-24.

[48] Quici N, Litter MI. Heterogeneous photocatalytic degradation of gallic acid under different experimental conditions. Photochem Photobiol Sci 2009; 8: 975-84.

[49] Emilio CA. Eliminación de ácidos oligocarboxílicos por Fotocatálisis Heterogénea y otras Tecnologías Avanzadas de Oxidación, PhD Thesis, Facultad de Ciencias Exactas y Naturales, Universidad de Buenos Aires, December 2006.

[50] Babay PA, Emilio CA, Ferreyra RE, Gautier EA, Gettar RT, Litter MI. Kinetics and mechanisms of EDTA photocatalytic degradation with TiO₂, Water Sci Technol 2001; 44: 179-85.

[51] Babay PA, Emilio CA, Ferreyra RE, Gautier EA, Gettar RT, Litter MI. Kinetics and mechanisms of EDTA photocatalytic degradation with TiO₂ under different experimental conditions. Int J Photoenergy 2001; 3:193-9.

[52] Malato S, Fernández-Ibáñez P, Maldonado MI, Blanco J, Gernjak W. Decontamination and disinfection of water by solar photocatalysis: Recent overview and trends. Catal Today 2009; 147: 1-59.

[53] Butters BE, Powell AL. System for photocatalytic treatment of contaminated media. US7008473B2, 2006.

[54] Carmignani GM, Frederick LW. Apparatus and method for photocatalytic purification and disinfection of water and ultrapure water. US6524447B1, 2003.

[55] Mozia S. Photocatalytic membrane reactors (PMRs) in water and wastewater treatment. A review. Separ Purif Technol 2010; 73: 71-91.

[56] Stefanelli ML. Photocatalytic membrane, process for its production and use thereof. EP1555064A1, 2005.

[57] Wang KH, Hsieh Y-H, Chao P-W, Cgang C-Y. The photocatalytic degradation of trichloroethane by chemical vapor deposition method prepared titanium dioxide catalyst. J Hazard Mater 2002; B25: 161-74.

[58] Kumakiri I, Bredesen R, Raeder H, Simon C. Photo-catalytic membrane reactor. WO2010021551A1, 2010.

[59] WATERCATOX, Waste Water Treatment by Catalytic Oxidation Contactor, A research project under the 5th Framework Programme of the European Commission, Contract no. EVK1-CT-2000-00073, http://www.sintef.no/units/matek/2420/242022/watercatox/ (Accessed on: May 28, 2010).

[60] Iojoiu, EE, Miachon S, Landrivon E, Walmsley JC, Ræder H, Dalmon J-A. Wet air oxidation in a catalytic membrane reactor: Model and industrial wastewater in single tubes and multichannel contactors. Appl Catal B 2007; 69: 196-206.

[61] Venegas Cabello PA, Yeber Ortis MC, Narvaez Dinamarca AL, del Pilar Sobenes Vennekool C, Ortiz Sanhueza CM. Photocatalytic reactor with a modular configuration and advanced oxidation process for purifying and disinfecting wastewater from aquaculture. EP1686095A1, 2006.

[62] Subrahmanyam M, Boule P, Valluri DK, Reddy MP, Noorjahan M, Raghaan KV. Method and apparatus for purification of industrial wastewater with thin film fixed bed TiO₂ photocatalyst. WO2004058649A1, 2004.

[63] Feng J, Yue PL, Hu X, Wong SKR. Synthesis of bentonite clay-based iron nanocomposite and its use as a heterogeneous photo Fenton catalyst. US20060076299A1, 2006.

[64] Subrahmanyam M, Kumari VD, Noorjahan M. Eco-friendly photo-Fenton catalyst-immobilized Fe(III) over HY-zeolite. US7407908B2, 2008.

[65] Sannino D, Ciambelli P, Ricciardi M, Isupova LA. Wastewater treatment by high efficiency heterogeneous photo-Fenton process. WO142724A1, 2008.

[66]   Borg C. Innovative treatment technologies for reclaimed water. WO2009017756, 2009.

[67]   Yarbrough ME, Takinen SA. System and method of reducing organic contaminants in feed water. US7531096B2, 2009.

[68]   Butters BE, Powell AL. Multi-barrier water purification system and method. WO2009044288A2, 2009.

[69]   Dos Santos AF, Caetano CA. Process for large amounts of wastewater desinfection and treatment, water recycling and utilization of organic and inorganic charges. WO2009135276A1, 2009.

[70]   Sahle-Demissie E, Pratim BP, Unnikrishnan RP, Chulhan K. Process using compact embedded electron induced ozonation and activation of nanostructured titanium dioxide photocatalyst for photocatalytic oxidation. US7691342B2, 2010.

[71]   Yan K, Hui H, Cui M, *et al.* Corona induced nonthermal plasmas: Fundamental study and industrial applications. J Electrostat 1998; 44: 17-39.

[72]   Yan K, van Heesch EJM, Pemen AJM, Huijbrechts AHJ. Elements of pulsed corona induced nonthermal plasmas for pollution control and sustainable development. J Electrostat 2001; 51-52: 218-24.

[73]   Grymonpre DR, Finney WC, Locke BR. Aqueous-phase pulsed streamer corona reactor using suspended activated carbon particles for phenol oxidation: model-data comparison. Chem Eng Sci 1999; 54: 3095-105.

[74]   Grymonpre, DR, Sharma AK, Finney WC, Locke BR. The role of Fenton's reaction in aqueous phase pulsed streamer corona reactors. Chem Eng J 2001; 82: 189-207.

[75]   Futamura S, Zhang AH, Yamamoto T. The dependence of nonthermal plasma behavior of VOCs on their chemical structures. J Electrostat 1997/98; 42: 51-62.

[76]   Fujii T, Rea M. Treatment of NO_x in exhaust gas by corona plasma over water surface. Vacuum 2000; 59: 228-35.

[77]   Bergendhal JA, Koryabkina N, Thompson RW. Methods and devices for the removal of organic contaminants from water. WO2007056717A2, 2007.